BLOOD COAGULATION REACTIONS
ON NANOSCALE MEMBRANE SURFACES

BY

VINCENT S. PUREZA

DISSERTATION

Submitted in partial fulfillment of the requirements
for the degree of Doctor of Philosophy in Biochemistry
in the Graduate College of the
University of Illinois at Urbana-Champaign, 2009

Urbana, Illinois

Doctoral Committee:

    Professor James Morrissey, Director of Research, Chair
    Professor Bradford Schwartz
    Professor Stephen Sligar
    Assistant Professor Emad Tajkhorshid

ABSTRACT

Blood coagulation requires the assembly of several membrane-bound protein complexes composed of regulatory and catalytic subunits. The biomembranes involved in these reactions not only provide a platform for these procoagulant proteins, but can also affect their function. Increased exposure of acidic phospholipids on the outer leaflet of the plasma membrane can dramatically modulate the catalytic efficiencies of such membrane-bound enzymes. Under physiologic conditions, however, these phospholipids spontaneously cluster into a patchwork of membrane microdomains upon which membrane binding proteins may preferentially assemble. As a result, the membrane composition surrounding these proteins is largely unknown. Through the development and use of a nanometer-scale bilayer system that provides rigorous control of the phospholipid membrane environment, I investigated the role of phosphatidylserine, an acidic phospholipid, in the direct vicinity (within nanometers) of two critical membrane-bound procoagulant protein complexes and their respective natural substrates. Here, I present how the assembly and function of the tissue factor·factor VIIa and factor Va·factor Xa complexes, the first and final cofactor·enzyme complexes of the blood clotting cascade, respectively, are mediated by changes in their immediate phospholipid environments.

Dedicated to my family

of knowledge, patience, and cookies. And to Andy Shaw for being an awesome collaborator.

I am sincerely indebted to those that made many of my experiments possible through their technical contributions. Many thanks to Guoyu Li and Julie Collins for their excellent TF preps. Liping Wang and Rachel Breitenfeld for their SPR advice. William Smith and Charles Zukoski for assistance with DLS. To Chad Rienstra and Zenmei Ohkubo for their continued support and always enlightening discussions. Many thanks to the members of the Biochemistry support staff: Louise Cox, Jeff Goldberg, Jeri Kyle and Jim Poepsel for making paperwork run so smoothly, no matter how many bumps that I may have put in the way. I also thank the AHA Predoctoral Fellowship for providing me with some of the financial means to complete this project.

Finally, to my mother and father, the most selfless and hardest working people I know, thank you for your unconditional love and support. To my brother Paul, a man of great character, thank you for your friendship, honesty and inspiration. To my pinsans, thanks for always giving me a home to go back to. To James Lee for some much-needed coffee and video game breaks, you help keep life and work in perspective. And to my fiancée, Linda Hasadsri: I love you, thank you for filling my world with your brilliant smile and making life that much more wonderful.

TABLE OF CONTENTS

NOTE OF CLARIFICATION

Portions of the following work will be submitted for publication or have already been published in the following manuscripts:

Pureza VS, Sligar SG, and Morrissey JH. Influence of the local phospholipid nanoenvironment on prothrombinase function. *In preparation*, 2009.

Morrissey JH, Pureza V, Davis-Harrison RL, Sligar SG, Rienstra CM, Kijac AZ, Ohkubo YZ and Tajkhorshid E. Protein-membrane interactions: blood clotting on nanoscale bilayers. *Journal of Thrombosis and Haemostasis*, 7 (Suppl. 1): 169-172, 2009.

Morrissey JH, Pureza V, Davis-Harrison RL, Sligar SG, Ohkubo YZ and Tajkhorshid E. Blood clotting reactions on nanoscale phospholipid bilayers. *Thrombosis Research*, 122 (Suppl. 1): S26-26, 2008.

Shaw AW*, Pureza VS*, Sligar SG, and Morrissey JH. The local phospholipid environment modulates the activation of blood clotting. *Journal of Biological Chemistry*, 282(9): 6556-6563, 2007. *Both authors contributed equally to the manuscript.

Portions of the following work also have been used to apply for US and PCT patents referenced below:

Morrissey JH, Sligar SG, and Pureza VS. Tissue factor compositions and methods. *US patent application*, Serial Number 11/259,950, October 2005.

Morrissey JH, Sligar SG, and Pureza VS. Tissue factor compositions and methods. *PCT patent application*, Serial Number PCT/US2005/38781, October 2005.

CHAPTER 1

INTRODUCTION

1.1   AN OVERVIEW OF BLOOD CLOTTING

At the macromolecular level, blood clotting is a series of proteolytic events in which zymogens are converted into active proteases (Fig. 1.1). This blood coagulation cascade requires the assembly of several phospholipid membrane-bound protein complexes that are made of a pair of regulatory and catalytic protein subunits. Blood clotting is initiated when a nonvascular integral membrane protein, tissue factor (TF), is exposed to the bloodstream. Once exposed to plasma, TF can complex with and significantly enhance the enzymatic activity of the serine protease factor VIIa (fVIIa). The resulting TF·VIIa complex then activates coagulation factors IX and X (fIX, fX, respectively) via the extrinsic pathway of blood coagulation. A series of proteolytic events ultimately lead to fibrin clot formation and platelet activation [1,2].

1.2   TISSUE FACTOR IS THE ACTIVATOR OF THE BLOOD COAGULATION CASCADE

TF is a small transmembrane cell surface protein responsible for the physiologic triggering of the blood coagulation cascade in normal hemostasis and the pathophysiologic activator of clotting in a variety of thrombotic diseases. TF initiates blood coagulation by interacting with the plasma protein, fVIIa. fVIIa has limited enzymatic activity on its own, but once bound to its protein cofactor, TF, its activity is tremendously enhanced [3]. The resulting TF·VIIa complex then

1

activates fIX and fX via limited proteolysis, ultimately leading to fibrin clot

formation and platelet activation. TF is constitutively expressed on many cell

types that are not in contact with blood, especially on the adventitial cells

surrounding most blood vessels. It can be thought of as forming a functional

hemostatic envelope around the vasculature to prevent excessive bleeding. TF

is also a component of atherosclerotic plaques, and TF-mediated coagulation

following plaque disruption is thought to trigger thrombus formation in myocardial

infarction and ischemic stroke [2].

TF can be found in either a 261 or a 263 amino acid form in the body with

nearly equal abundance. These two species have a molecular weight of 29,447

or 29,593 Da respectively [1], but have an apparent molecular weight of

approximately 45,000 Da when analyzed by sodium dodecyl sulfate (SDS) gel

electrophoresis due to post-translational glycosylation [4]. Glycosylation has

been found unnecessary for procoagulant activity and fully active, recombinant

TF is routinely produced in bacteria. The structure of TF protein consists of an

extracellular domain, a single transmembrane domain, and a short cytoplasmic

tail which respectively participate in fVII(a) binding, cell membrane anchoring,

and an uncertain function (Fig. 1.2). Deletion of the cytoplasmic tail has no

evident effect on procoagulant activity [5], but is speculated to play a role in cell

signaling events [6]. TF must be incorporated into a membrane bilayer that

includes net negatively-charged phospholipids, in particular phosphatidylserine

(PS), for maximal procoagulant activity [7,8]. This reliance on phospholipids is

2

evident with recombinant forms of TF that lack a transmembrane domain (soluble TF or sTF). Although sTF is able to bind fVIIa, the resulting sTF·VIIa complex exhibits dramatically decreased rates of substrate activation [9].

The mechanism(s) by which TF enhances the activity of fVIIa, and the role of specific phospholipids in enhancing catalysis by TF·VIIa are not fully understood. It is believed that membrane-bound TF: 1) provides a receptor-like surface for binding its substrates [10,11], 2) allosterically activates fVIIa via induction of conformational change within the fVIIa active site [7], and 3) rests on a phospholipid surface that is also conducive to binding substrates [8], effectively increasing the concentration of substrates within the vicinity of TF. The combined result of these interactions conferred by TF increases the activity of fVIIa many thousand-fold [10-12].

1.3   VITAMIN K-DEPENDENT PROTEINS OF BLOOD CLOTTING BIND MEMBRANES VIA γ-CARBOXYGLUTAMIC ACID DOMAINS

Many blood coagulation proteins such as prothrombin, fVII, factor IX and fXa belong to a highly homologous family of vitamin K-dependent proteins (Fig. 1.2). Vitamin K-dependent proteins are so-named because certain N-terminal Glu residues in these proteins are post-translationally modified into γ-carboxyglutamic acid (Gla) residues via a vitamin K-dependent carboxylation reaction [13]. In the presence of Ca^{2+}, this Gla-containing domain (Gla domain) enables these plasma proteins to reversibly bind certain phospholipid membranes [14,15]. These proteins are predominantly synthesized in the liver

3

and are first released as zymogens into the bloodstream. They are then proteolytically cleaved into their active, "a", forms under certain physiologic and pathophysiologic conditions. The half-lives of the activated forms, however, last merely seconds due to the presence of many protease inhibitors in the circulation. fVIIa, on the other hand has limited reactively with these compounds and can persist in plasma for hours [16].

These serine proteases demonstrate trypsin-like homology via the Ser-His-Asp catalytic triad. Unlike more canonical serine endopeptidases like trypsin and elastase, however, these active blood coagulation proteases require a suitable phospholipid membrane, Ca^{2+} and a protein cofactor for optimal activity. For example, fVII is the zymogen precursor of fVIIa, and fVIIa complexes with TF in the presence of phospholipids and Ca^{2+} to make TF·VIIa, a highly active protein cofactor·enzyme complex.

1.3.1 The Structure and Function of Factors VII and VIIa

fVII is a 416 amino acid glycoprotein with a molecular weight of 50,000 Da [17]. This zymogen is composed of two epidermal growth factor (EGF)-like domains, a serine protease precursor domain and a Gla domain (Fig. 1.2). Within its Gla domain, 10 γ-carboxyglutamatic acid residues are present [18]. The plasma concentration of fVII is approximately 10 nM [17,19]. Upon limited proteolysis, fVII is converted to an activated serine protease called fVIIa. The conversion of fVII to fVIIa is due to cleavage of a single peptide bond, Arg152-Ile, and can be accomplished by several proteases such as thrombin, fIXa, fXa, fXIIa

4

and TF complexed with fVIIa itself [20-22]. Unlike other circulating activated serine proteases, fVIIa has a relatively long plasma half-life [16]. As such, when TF is exposed, the trace amounts of fVIIa that are present in the bloodstream are thought to prime the blood clotting cascade [23]. fVIIa has very limited proteolytic activity on its own, but when complexed with TF, Ca^{2+} and a suitable phospholipid membrane, its ability to activate fIX and fX increases substantially [3].

1.3.2 The Structure and Function of Factors X and Xa

fX is a substrate for the TF·VIIa complex. It is a 488 amino acid glycoprotein with a molecular weight of 56,000 Da [17]. This zymogen is composed of two EGF-like domains, a serine protease precursor domain and a Gla domain (Fig. 1.2). It has 11 γ-carboxyglutamatic acid residues that are present in its Gla domain [24], and the plasma concentration of fX is approximately 200 nM [17,25]. The conversion of fX to its activated form, fXa, is due to a cleavage at Arg194-Ile, catalyzed by either TF·VIIa or the factor VIIIa·factor IXa complex [26]. fXa combines with its protein cofactor factor Va (fVa) to form the Va·Xa complex, which is responsible for catalyzing the conversion of prothrombin to thrombin.

1.3.3 The Structure and Function of Prothrombin

Prothrombin, also known as factor II, is a 579 amino acid glycoprotein with a molecular weight of 72,000 Da [17]. This zymogen is composed of two kringle

structures, a serine protease precursor domain and a Gla domain [27]. Ten γ-carboxyglutamatic acid residues are present in its Gla domain, and the plasma concentration of prothrombin is between 1 and 2 μM [17,28]. Prothrombin is converted by the Va·Xa complex to its major product, α-thrombin (thrombin), through sequential proteolytic cleavage at two sites, Arg284-Thr and Arg320-Ile (Fig. 1.2). Cleavage at the Arg320-Ile activates the protease domain of prothrombin. Alternatively, cleavage at Arg284-Thr removes the Gla domain from the protein rendering it soluble. Depending on the order of cleavage of these two bonds, two possible intermediates, meizothrombin, or prethrombin 2, may be formed [29]. Meizothrombin is the predominant or possibly only physiologically-relevant intermediate formed from the Va·Xa complex conversion of prothrombin to thrombin [30]; it is transiently formed when cleavage at Arg320-Ile precedes that of Arg284-Thr in the presence of a proper membrane surface.

1.4   THE STRUCTURE AND FUNCTION OF FACTORS V AND Va

Factor V (fV) is the procofactor form of fVa (Fig. 1.4). As opposed to the Gla domain-containing proteins discussed above, the membrane binding domains of fV most closely resemble factor VIII and to a lesser extent, ceruloplasmin or discoidin I [31-33]. fV is a 2,196 amino acid protein with a molecular weight of 330,000 Da [17]. It has a plasma concentration of approximately 30 nM [17,25], of which 20 to 25% are found in α-granules of platelets [34]. It is organized into 6 domains: A1-A2-B-A3-C1-C2 [32]. In order to function as a cofactor, fV is proteolytically cleaved by thrombin at residues

6

Arg709-Ser, Arg1018-Thr, and Arg1545-Ser [32]. As a result, the B domain is

removed and its activated form, fVa, composed of a light and heavy chain, is

formed. The heavy chain (94,000 Da) and light chain (74,000 Da) of fVa are

noncovalently linked through a Ca^{2+} bridge [35]. Prothrombin interacts with the

light chain, and fXa interacts with both the heavy and light chains. The heavy

chain confers most of the cofactor activity and the light chain (A3-C1-C2)

constitutes the primary membrane binding domain for fVa [36,37]. Within the

light chain, the C1 and C2 domains (C domains) are generally regarded as the

primary membrane binding domains of fVa [38-41]. The exact contribution of the

A3 domain to phospholipid binding is still relatively unknown. This domain has

been recently modeled resting away from the membrane and upon the C

domains, but other studies have also shown it interacting with phospholipids

[39,42]. The fVa molecule binds membranes via electrostatic and hydrophobic

interactions through an incompletely understood mechanism [37,43,44]. Under

experimental conditions, fVa is able bind membranes composed of pure PC,

however the physiological relevance of this is questionable as the reported K_d for

this is at least 2 orders of magnitude beyond the reported plasma concentration

of fVa [34,45]. As such, to achieve binding at physiological levels, a minimum

amount of PS molecules is simply required.

1.5　Va·Xa IS THE FINAL COFACTOR·PROTEASE COMPLEX OF BLOOD COAGULATION

The Va·Xa complex (prothrombinase complex) is the physiological catalyst responsible for the conversion of prothrombin to thrombin [46,47]. This complex is composed of a serine protease, fXa, and its protein cofactor, fVa, assembled upon a membrane surface containing anionic phospholipids and Ca^{2+} [48,49]. Membrane-bound fVa is thought to provide an anchor for both its companion protease, fXa, and its substrate, prothrombin [35]. Studies using liposomes and other model membranes have shown that anionic phospholipids are required for optimal prothrombinase activity, with PS playing the most active role [50,51]. Unfortunately, the mechanisms by which PS enhances the enzymatic activity of prothrombinase – or any other protease-cofactor complex in blood clotting – are not fully understood.

1.6　THROMBIN PLAYS A CENTRAL ROLE IN HEMOSTASIS

Thrombin, or α-thrombin, is a soluble serine protease derived from the Va·Xa-catalyzed cleavage of prothrombin. It has a molecular weight of 36,000 Da and plays a central role in many physiological processes involving the overall maintenance of blood coagulation. These processes include, but are not limited to, the activation of various zymogens and cofactors, the activation of platelets and the formation of fibrin from fibrinogen [35]. This fibrin clot is the end-result of the blood coagulation cascade and is further stabilized through the actions of activated factor XIII (fXIIIa). fXIIIa is a transglutaminase that catalyzes covalent

bond formation between lysine and glutamine residues on fibrin that effectively cross-links and strengthens the fibrin clot. In the laboratory, preparations of thrombin are susceptible to degradation via contaminating proteases (possibly including, thrombin itself). These degraded forms of thrombin have relatively distinct cleavages patterns. In general, these so-called β and γ-thrombins have limited activity towards fibrinogen and other natural substrates [52].

1.7   PHOSPHOLIPID MEMBRANES ARE THE SITES OF BLOOD CLOTTING REACTIONS

Cell surfaces such as activated platelets, monocytes and damaged endothelial cells constitute the membrane surfaces for blood clotting reactions, *in vivo* [51]. On a resting cell or unactivated platelet surface, PS and other aminophospholipids are normally sequestered within plasma membranes and away from the circulation, while choline phospholipids such as phosphatidylcholine (PC) are predominantly on the outer leaflet [48,53]. Upon cell damage or induction of other stressors, anionic lipids such as PS, are scrambled onto the outer leaflet. The end result of this process ultimately induces many events in the body, including blood clotting.

To great effect, many *in vitro* studies involving blood clotting complexes have used mixtures of net neutral and anionic phospholipids in liposomes as model membrane systems that recapitulate the stimulatory affects of their natural counterparts [50,51]. Notably, PS is accepted as the most effective surface in supporting catalysis [51]. Conventional phospholipid preparations containing

high concentrations of PS, however, are susceptible to fusion or collapse, in the presence of physiological amounts of Ca^{2+} [54]. As such, mixtures of PS and the net neutral phospholipid, PC (together as PCPS) are routinely used in experiments.

In the presence of Ca^{2+} or membrane binding proteins, even simple membranes composed of binary mixtures of net-anionic and neutral phospholipids are capable of forming microdomains rich in anionic phospholipids. Experiments with giant unilaminellar vesicles, for example, have shown that anionic phospholipids are capable of migrating across relatively long distances and clustering into large microdomains [55,56]. Heterogeneous domain formation may, in turn, substantially change the local surface properties on the membrane surface. As a result, the actual phospholipid microenvironment on mixed-phospholipid membranes may vary dramatically from the average composition of the bulk membrane. Little is known, however, about how local membrane microdomain composition affects the assembly and function of procoagulant protein complexes.

TF is an integral membrane protein and must be incorporated into a suitable membrane surface for optimal function. Most methods for inserting TF into liposomes (TF-liposomes) involve the formation of mixed micelles containing detergent, phospholipids and TF, taking advantage of the natural ability of phospholipids to self-assemble into bilayer structures upon detergent removal. Although our laboratory has recently developed a rapid method by which TF can

10

be incorporated into liposomes [57], some of the traditional problems associated with classic TF relipidation techniques still remain, such as: 1) random orientation of TF in the liposomes, with roughly half of the molecules facing into the lumen; 2) heterogeneity in TF-liposome size distribution; and 3) inconsistent loading of TF from one liposome to another.

An additional difficulty in using TF-liposomes to study the function of the TF·VIIa complex is that both the enzyme (fVIIa) and the substrates bind reversibly to the phospholipid surface independent of their interactions with TF. As such, there is a large excess of protein binding sites on the liposome surface compared with the surface density of TF. This makes it technically difficult to distinguish between protein-phospholipid and protein-protein interactions when studying the assembly and function of protease-cofactor pairs.

1.8 NANODISCS PROVIDE RIGOROUS CONTROL OF THE LIPID NANOENVIRONMENT SURROUNDING PROCOAGULANT PROTEINS

In the present study, we used nanometer-scale phospholipid bilayers (Nanodiscs) of defined size and phospholipid composition as the experimental membrane surface upon which to assemble and study the components of the blood coagulation cascade (Fig. 1.5). Nanodiscs are water-soluble bilayers encircled and stabilized by an amphipathic helical protein termed membrane scaffold protein (MSP). The nanobilayers within Nanodiscs are monodisperse and exhibit lipid fluidity comparable to liposomes [58,59]. Nanodiscs self-assemble from mixtures of phospholipids and MSP, to form stabilized nanoscale

11

bilayers whose lipid composition is under strict experimental control. Newer-generation Nanodiscs have been developed using MSPs that have been systematically elongated or truncated to yield stabilized, monodisperse phospholipid bilayers ranging from about 8 to 15 nm in diameter [60]. By assembling the constituent proteins of certain blood clotting complexes on these nanobilayers, we can circumvent the long-range recruitment of anionic phospholipids that occurs in larger phospholipid systems such as liposomes. This affords us complete control over the composition of the membrane nanoenvironment immediately surrounding these complexes.

1.9   BLOOD COAGULATION ON NANOSCALE MEMBRANE SURFACES

Blood coagulation requires the assembly of several membrane-bound protein complexes, each composed of both regulatory and catalytic protein subunits. In addition to providing a platform for assembly, biological membranes also modulate the catalytic activity of serine protease-cofactor complexes in blood clotting [51]. Studies using liposomes and other model membranes have shown that anionic phospholipids are required for optimal procoagulant activity, with PS being the most active [50,51]. Unfortunately, the mechanisms by which PS enhances the enzymatic activity of protease-cofactor complexes in blood clotting are not fully understood.

I hypothesize that blood clotting protease-cofactor complexes partition into discrete membrane microdomains of very high PS content. Studies of giant unilaminellar vesicles composed of mixtures of anionic and neutral phospholipids

have shown that plasma concentrations of Ca^{2+} can induce anionic phospholipids to move over relatively long distances to cluster into anionic phospholipid-rich membrane domains. Clustering of anionic phospholipids was even more dramatic when vesicles were treated with combinations of Ca^{2+} and proteins known to bind to anionic phospholipids, such that the membrane-binding proteins co-clustered with anionic phospholipids [55,56]. It therefore seems likely that blood clotting reactions occur preferentially on membrane surfaces containing very high amounts of PS in the immediate vicinity, which may result from both Ca^{2+} and the PS-binding properties of the proteins themselves. Unfortunately, when using even simple model membranes, it is very difficult to know the phospholipid composition immediately surrounding these membrane-bound complexes and their membrane-bound substrates. For example, in the presence of plasma concentrations of Ca^{2+}, liposomes composed of 20% PS and 80% PC are likely to segregate into a patchwork of microenvironments in which the local PS content at any given point may be considerably higher or lower than the average of 20%. Thus, local variations in the membrane nanoenvironment immediately surrounding these complexes may dramatically alter their catalytic efficiencies. When using liposomes or other model membranes, this parameter is typically not under experimental control.

To address this problem, I have used nanometer-scale phospholipid bilayers (Nanodiscs) of defined size and phospholipid composition as the experimental membrane surface upon which to assemble and study the

components of two critical procoagulant complexes: TF·VIIa and 2) Va·Xa.

These are the first and last membrane-dependent complexes in the coagulation

cascade respectively. By assembling the constituent proteins of these two

complexes on nanoscale bilayers, the long-range recruitment of anionic

phospholipids that occurs in larger phospholipid systems such as liposomes can

be circumvented. This affords complete control over the composition of the

membrane nanoenvironment immediately surrounding (within nanometers) of

these complexes. This first chapter serves as a brief introduction to blood

coagulation and the dynamic role of membrane micro- and even submicroscopic

environments in shaping this process. The second chapter of this thesis

illustrates the assembly and characterization of Nanodiscs containing anionic

phospholipids and then details the incorporation of TF into these structures.

Using the same nanoscale system, the third chapter describes the assembly and

function of the TF·VIIa complex, the initiator of the blood clotting cascade. The

fourth chapter then investigates the Va·Xa complex, the final phospholipid-

dependent complex of the blood coagulation system. Finally, the fifth chapter will

summarize and discuss the relevance of this project as it relates to the overall

process of blood coagulation, as well as the potential clinical applications of this

work.
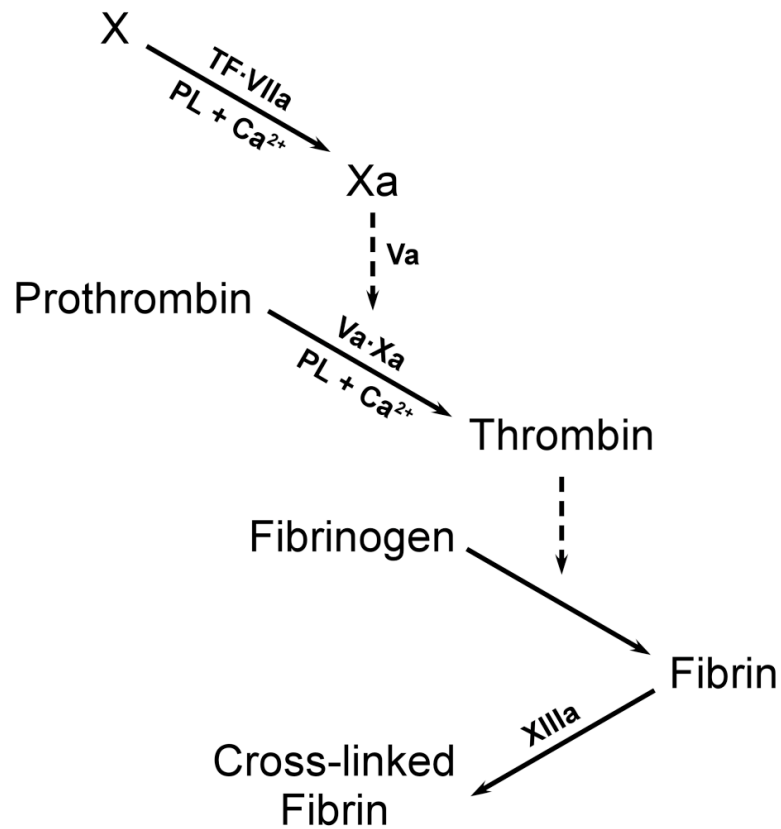
FIGURE 1.1 Simplified TF·VIIa coagulation pathway. Blood coagulation is a series of proteolytic events where zymogens are converted into active proteases. TF·VIIa converts factor X to factor Xa. Factor Xa complexes with factor Va to form Va·Xa. Va·Xa converts prothrombin to thrombin. Thrombin converts fibrinogen to fibrin, and factor XIIIa catalyzes the cross-linking of fibrin. The two membrane-bound protein complexes depicted in this figure are made of protein cofactor·protease partners that require calcium ions (Ca^{2+}) and phospholipids (PL) for maximal activity.
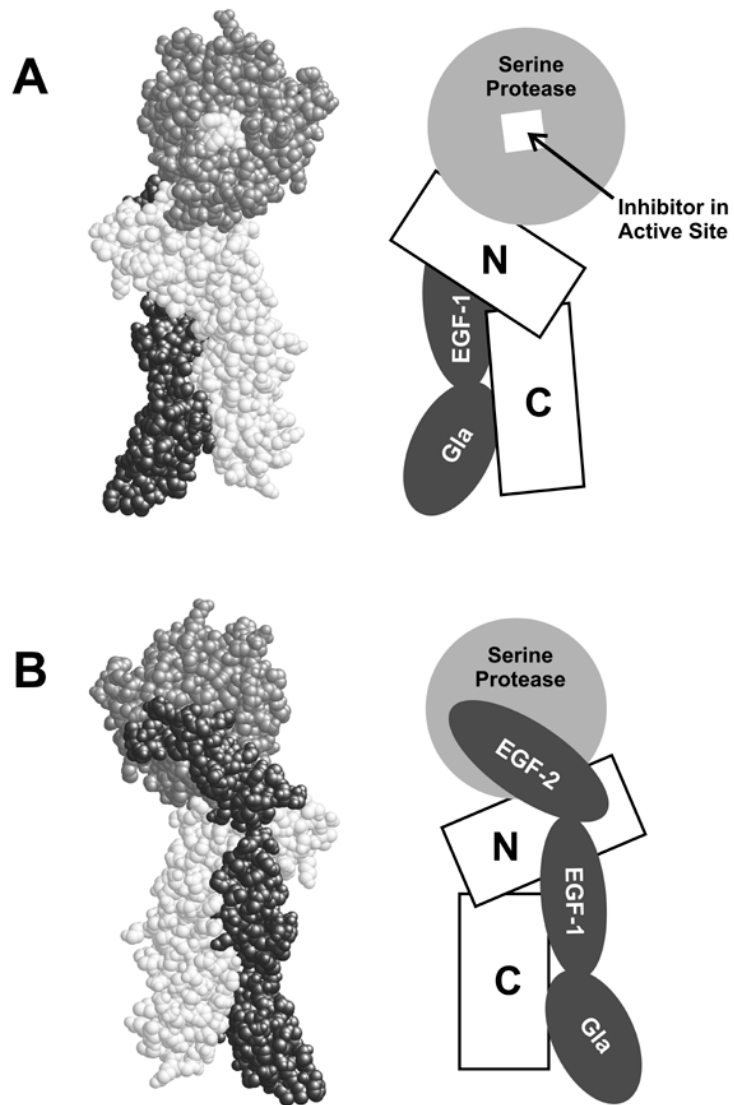
FIGURE 1.2 Structure of the soluble TF·VIIa complex. The crystal structure is on the left, and a cartoon is on the right. The active site of factor VIIa is depicted toward (A) and away from (B) the viewer. Depicted on factor VIIa is its serine protease domain (*light gray*) and its EGF and Gla domains (*dark gray*). The inhibitor (*white*) is in the active site of factor VIIa. TF, with its labeled N and C termini, is also *white*. The transmembrane domain and cytoplasmic tail of TF is not present in this figure, and the membrane surface would be located at the bottom of each complex. (Generated from file "1DAN" from the Protein Data Bank, courtesy of James Morrissey.)

Factor VII   (50 kDa)

Arg 152

Gla – EGF – EGF — Serine Protease

S – S

Factor X   (56 kDa)

Arg 194

Gla – EGF – EGF — Serine Protease

S – S

Prothrombin   (72 kDa)

Arg 284   Arg 320

Gla — Kringle — Kringle — Serine Protease

S – S
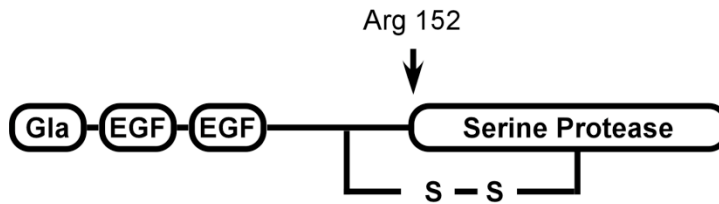
FIGURE 1.3 Vitamin K-dependent coagulation factors. Schematic representations of γ-carboxyglutamic acid residue (Gla)-containing zymogens of blood clotting: factor VII, X and prothrombin. Both factor VII and X contain epidermal growth factor (EGF)-like domains, while prothrombin has kringle domains. Arrows indicate location of cleavage sites that are needed to generate an active serine protease.

17
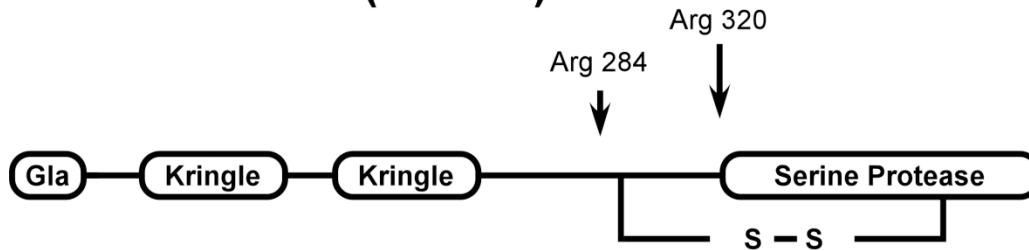
Factor V   (330 kDa)

Arg 709   Arg 1018   Arg 1545

A1   A2   B   A3   C1   C2
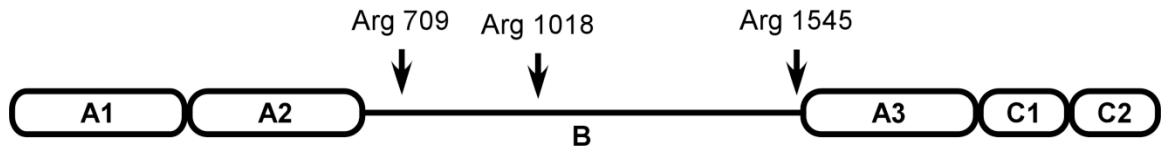
FIGURE 1.4 Schematic representation of procofactor, factor V. Labeled is the heavy chain (A1, A2) and the light chain (A3, C1, C2), held together by the B domain. Arrows indicate location of cleavage sites needed to generate an active protein cofactor. Complete cleavage by thrombin releases the B domain and produces activated factor V consisting of its heavy and light chains held noncovalently by Ca^{2+}.

5.5 nm

**Phospholipid bilayer diameter
8 to 15 nm**
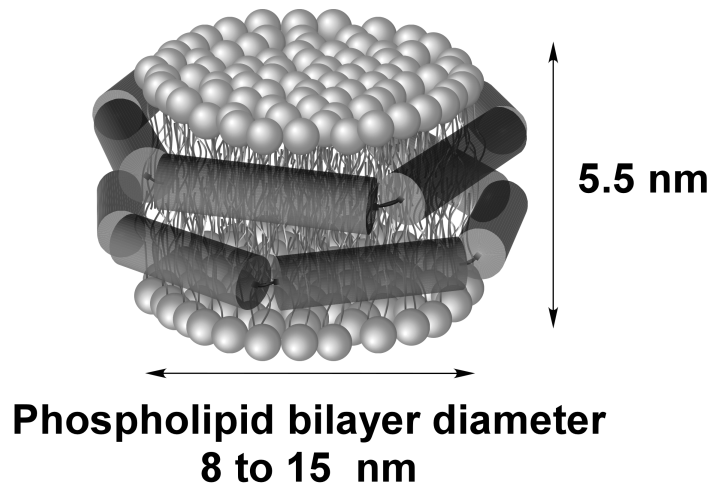
FIGURE 1.5 Cartoon representation of a Nanodisc. Nanodiscs are water-soluble bilayers encircled and stabilized by an amphipathic helical protein termed membrane scaffold protein (MSP). MSPs have been systematically elongated or truncated to yield stabilized, monodisperse phospholipid bilayers ranging from about 8 to 15 nm in diameter. Depicted are phospholipids in *light gray* and MSPs in *dark gray*.

1.11   REFERENCES

1. Morrissey JH, Mutch NJ. Tissue factor structure and function. In: Colman RW, Marder VJ, Clowes AW, George JN, Goldhaber SZ (editors). *Hemostasis and Thrombosis: Basic Principles and Clinical Practice.* Philadelphia: Lippincott Williams and Wilkins, 2006; 91-106.

2. Eilertsen KE, Osterud B. Tissue factor: (patho)physiology and cellular biology. *Blood Coagul Fibrinolysis* 2004; **15:** 521-538.

3. Wildgoose P, Jorgensen T, Komiyama Y, Nakagaki T, Pedersen A, Kisiel W. The role of phospholipids and the factor VII Gla-domain in the interaction of factor VII with tissue factor. *Thromb Haemost* 1992; **67:** 679-685.

4. Pittman DD, Tomkinson KN, Kaufman RJ. Post-translational requirements for functional factor V and factor VIII secretion in mammalian cells. *J Biol Chem* 1994; **269:** 17329-17337.

5. Paborsky LR, Caras IW, Fisher KL, Gorman CM. Lipid association, but not the transmembrane domain, is required for tissue factor activity. Substitution of the transmembrane domain with a phosphatidylinositol anchor. *J Biol Chem* 1991; **266:** 21911-21916.

6. Rao LV, Pendurthi UR. Tissue factor-factor VIIa signaling. *Arterioscler Thromb Vasc Biol* 2005; **25:** 47-56.

7. Huang Q, Neuenschwander PF, Rezaie AR, Morrissey JH. Substrate recognition by tissue factor-factor VIIa. Evidence for interaction of residues Lys165 and Lys166 of tissue factor with the 4-carboxyglutamate-rich domain of factor X. *J Biol Chem* 1996; **271:** 21752-21757.

8. Rezaie AR, Neuenschwander PF, Morrissey JH, Esmon CT. Analysis of the functions of the first epidermal growth factor-like domain of factor X. *J Biol Chem* 1993; **268:** 8176-8180.

9. Fiore MM, Neuenschwander PF, Morrissey JH. The biochemical basis for the apparent defect of soluble mutant tissue factor in enhancing the proteolytic activities of factor VIIa. *J Biol Chem* 1994; **269:** 143-149.

10. Komiyama Y, Pedersen AH, Kisiel W. Proteolytic activation of human factors IX and X by recombinant human factor VIIa: effects of calcium, phospholipids, and tissue factor. *Biochemistry* 1990; **29:** 9418-9425.

11. Bom VJ, Bertina RM. The contributions of Ca2+, phospholipids and tissue-factor apoprotein to the activation of human blood-coagulation factor X by activated factor VII. *Biochem J* 1990; **265:** 327-336.

12. Nemerson Y, Gentry R. An ordered addition, essential activation model of the tissue factor pathway of coagulation: evidence for a conformational cage. *Biochemistry* 1986; **25:** 4020-4033.

13. Stafford DW. The vitamin K cycle. *J Thromb Haemost* 2005; **3:** 1873-1878.

14. Krishnaswamy S, Walker RK. Contribution of the prothrombin fragment 2 domain to the function of factor Va in the prothrombinase complex. *Biochemistry* 1997; **36:** 3319-3330.

15. Mann KG. Prothrombin. *Methods Enzymol* 1976; **45:** 123-156.

16. Kondo S, Kisiel W. Regulation of factor VIIa activity in plasma: evidence that antithrombin III is the sole plasma protease inhibitor of human factor VIIa. *Thromb Res* 1987; **46:** 325-335.

17. Furie B, Furie BC. The molecular basis of blood coagulation. *Cell* 1988; **53:** 505-518.

18. Di Scipio RG, Hermodson MA, Yates SG, Davie EW. A comparison of human prothrombin, factor IX (Christmas factor), factor X (Stuart factor), and protein S. *Biochemistry* 1977; **16:** 698-706.

19. Fair DS. Quantitation of factor VII in the plasma of normal and warfarin-treated individuals by radioimmunoassay. *Blood* 1983; **62:** 784-791.

20. Masys DR, Bajaj SP, Rapaport SI. Activation of human factor VII by activated factors IX and X. *Blood* 1982; **60:** 1143-1150.

21. Bajaj SP, Rapaport SI, Brown SF. Isolation and characterization of human factor VII. Activation of factor VII by factor Xa. *J Biol Chem* 1981; **256:** 253-259.

22. Radcliffe R, Nemerson Y. Activation and control of factor VII by activated factor X and thrombin. Isolation and characterization of a single chain form of factor VII. *J Biol Chem* 1975; **250:** 388-395.

23. Mann KG, Krishnaswamy S, Lawson JH. Surface-dependent hemostasis. *Semin Hematol* 1992; **29:** 213-226.

24. McMullen BA, Fujikawa K, Kisiel W, Sasagawa T, Howald WN, Kwa EY, Weinstein B. Complete amino acid sequence of the light chain of human blood coagulation factor X: evidence for identification of residue 63 as beta-hydroxyaspartic acid. *Biochemistry* 1983; **22:** 2875-2884.

25. Kane WH, Davie EW. Blood coagulation factors V and VIII: structural and functional similarities and their relationship to hemorrhagic and thrombotic disorders. *Blood* 1988; **71:** 539-555.

26. Baugh RJ, Krishnaswamy S. Role of the activation peptide domain in human factor X activation by the extrinsic Xase complex. *J Biol Chem* 1996; **271:** 16126-16134.

27. Degen SJ, MacGillivray RT, Davie EW. Characterization of the complementary deoxyribonucleic acid and gene coding for human prothrombin. *Biochemistry* 1983; **22:** 2087-2097.

28. McDuffie FC, Giffin C, Niedringhaus R, Mann KG, Owen CA, Jr., Bowie EJ, Peterson J, Clark G, Hunder GG. Prothrombin, thrombin and prothrombin fragments in plasma of normal individuals and of patients with laboratory evidence of disseminated intravascular coagulation. *Thromb Res* 1979; **16:** 759-773.

29. Krishnaswamy S, Mann KG, Nesheim ME. The prothrombinase-catalyzed activation of prothrombin proceeds through the intermediate meizothrombin in an ordered, sequential reaction. *J Biol Chem* 1986; **261:** 8977-8984.

30. Walker RK, Krishnaswamy S. The activation of prothrombin by the prothrombinase complex. The contribution of the substrate-membrane interaction to catalysis. *J Biol Chem* 1994; **269:** 27441-27450.

31. Takahashi N, Bauman RA, Ortel TL, Dwulet FE, Wang CC, Putnam FW. Internal triplication in the structure of human ceruloplasmin. *Proc Natl Acad Sci U S A* 1983; **80:** 115-119.

32. Kane WH, Davie EW. Cloning of a cDNA coding for human factor V, a blood coagulation factor homologous to factor VIII and ceruloplasmin. *Proc Natl Acad Sci U S A* 1986; **83:** 6800-6804.

33. Ortel TL, Takahashi N, Putnam FW. Structural model of human ceruloplasmin based on internal triplication, hydrophilic/hydrophobic character, and secondary structure of domains. *Proc Natl Acad Sci U S A* 1984; **81:** 4761-4765.

34. Tracy PB, Eide LL, Bowie EJ, Mann KG. Radioimmunoassay of factor V in human plasma and platelets. *Blood* 1982; **60:** 59-63.

35. Jenny NS, Lundblad RL, Mann KG. Thrombin. In: Colman RW, Marder VJ, Clowes AW, George JN, Goldhaber SZ (editors). *Hemostasis and Thrombosis: Basic Principles and Clinical Practice.* Philadelphia: Lippincott Williams and Wilkins, 2006; 193-213.

36. van de Waart P, Bruls H, Hemker HC, Lindhout T. Interaction of bovine blood clotting factor Va and its subunits with phospholipid vesicles. *Biochemistry* 1983; **22:** 2427-2432.

37. Tracy PB, Mann KG. Prothrombinase complex assembly on the platelet surface is mediated through the 74,000-dalton component of factor Va. *Proc Natl Acad Sci U S A* 1983; **80:** 2380-2384.

38. Ortel TL, Devore-Carter D, Quinn-Allen M, Kane WH. Deletion analysis of recombinant human factor V. Evidence for a phosphatidylserine binding site in the second C-type domain. *J Biol Chem* 1992; **267:** 4189-4198.

39. Kalafatis M, Jenny RJ, Mann KG. Identification and characterization of a phospholipid-binding site of bovine factor Va. *J Biol Chem* 1990; **265:** 21580-21589.

40. Kalafatis M, Rand MD, Mann KG. Factor Va-membrane interaction is mediated by two regions located on the light chain of the cofactor. *Biochemistry* 1994; **33:** 486-493.

41. Gilbert GE, Baleja JD. Membrane-binding peptide from the C2 domain of factor VIII forms an amphipathic structure as determined by NMR spectroscopy. *Biochemistry* 1995; **34:** 3022-3031.

42. Kalafatis M, Xue J, Lawler CM, Mann KG. Contribution of the heavy and light chains of factor Va to the interaction with factor Xa. *Biochemistry* 1994; **33:** 6538-6545.

43. Pusey ML, Mayer LD, Wei GJ, Bloomfield VA, Nelsestuen GL. Kinetic and hydrodynamic analysis of blood clotting factor V-membrane binding. *Biochemistry* 1982; **21:** 5262-5269.

44. Pusey ML, Nelsestuen GL. Membrane binding properties of blood coagulation Factor V and derived peptides. *Biochemistry* 1984; **23:** 6202-6210.

45. Koppaka V, Lentz BR. Binding of bovine factor Va to phosphatidylcholine membranes. *Biophys J* 1996; **70:** 2930-2937.

46. Mann KG. The assembly of blood clotting complexes on membranes. *Trends in Biochemical Sciences* 1987; **12:** 229-233.

47. Mann KG. How much factor V is enough? *Thromb Haemost* 2000; **83:** 3-4.

48. Zwaal RF. Membrane and lipid involvement in blood coagulation. *Biochim Biophys Acta* 1978; **515:** 163-205.

49. Mann KG, Nesheim ME, Church WR, Haley P, Krishnaswamy S. Surface-dependent reactions of the vitamin K-dependent enzyme complexes. *Blood* 1990; **76:** 1-16.

50. Castellino FJ. Human Protein C and Activated Protein C - Components of the Human Anticoagulation System. *Trends in Cardiovascular Medicine* 1995; **5:** 55-62.

51. Mann KG, Jenny RJ, Krishnaswamy S. Cofactor proteins in the assembly and expression of blood clotting enzyme complexes. *Annu Rev Biochem* 1988; **57:** 915-956.

52. Lundblad RL, Nesheim ME, Straight DL, Sailor S, Bowie J, Jenzano JW, Roberts JD, Mann KG. Bovine alpha- and beta-thrombin. Reduced fibrinogen-clotting activity of beta-thrombin is not a consequence of reduced affinity for fibrinogen. *J Biol Chem* 1984; **259:** 6991-6995.

53. Schroit AJ, Zwaal RF. Transbilayer movement of phospholipids in red cell and platelet membranes. *Biochim Biophys Acta* 1991; **1071:** 313-329.

54. Wilschut J, Duzgunes N, Hoekstra D, Papahadjopoulos D. Modulation of membrane fusion by membrane fluidity: temperature dependence of divalent cation induced fusion of phosphatidylserine vesicles. *Biochemistry* 1985; **24:** 8-14.

55. Haverstick DM, Glaser M. Visualization of Ca2+-induced phospholipid domains. *Proc Natl Acad Sci U S A* 1987; **84:** 4475-4479.

56. Yang L, Glaser M. Formation of membrane domains during the activation of protein kinase C. *Biochemistry* 1996; **35:** 13966-13974.

57. Smith SA, Morrissey JH. Rapid and efficient incorporation of tissue factor into liposomes. *J Thromb Haemost* 2004; **2:** 1155-1162.

58. Shaw AW, McLean MA, Sligar SG. Phospholipid phase transitions in homogeneous nanometer scale bilayer discs. *FEBS Lett* 2004; **556:** 260-264.

59. Denisov IG, McLean MA, Shaw AW, Grinkova YV, Sligar SG. Thermotropic phase transition in soluble nanoscale lipid bilayers. *J Phys Chem B* 2005; **109:** 15580-15588.

60. Denisov IG, Grinkova YV, Lazarides AA, Sligar SG. Directed self-assembly of monodisperse phospholipid bilayer Nanodiscs with controlled size. *J Am Chem Soc* 2004; **126:** 3477-3487.

CHAPTER 2

ASSEMBLY AND CHARACTERIZATION OF NANOSCALE BILAYERS

2.1   BACKGROUND

Blood coagulation requires the assembly of membrane-binding protein complexes composed of catalytic (protease) and regulatory subunits. Cells such as platelets can dramatically mediate the catalytic efficiencies of such lipid-binding proteases through increased exposure of PS on the outer leaflet of the plasma membrane. In the presence of Ca^{2+}, anionic phospholipids such as PS spontaneously cluster into membrane microdomains upon which phospholipid-binding proteins may preferentially assemble. Studies of giant unilamellar vesicles composed of mixtures of anionic and neutral phospholipids have shown that normal plasma concentrations of Ca^{2+} can induce such clustering of anionic phospholipids over relatively long distances. This phenomenon was further attenuated by the addition of proteins known to bind to anionic phospholipids [1,2].

It therefore seems likely that blood clotting reactions occur preferentially on membrane surfaces containing locally high PS content, which may result from both Ca^{2+} and the PS-binding properties of the proteins themselves. Unfortunately, even when using simple model membranes, it is very difficult to know the phospholipid composition immediately surrounding the membrane-bound complexes of blood clotting. In the presence of physiological plasma concentrations of Ca^{2+}, for example, liposomes composed of 20% PS and 80%

25

PC are likely to segregate into a patchwork in which the local PS content at any given point may be considerably higher or lower than the average of 20%. Thus, local variations in the membrane nanoenvironment immediately surrounding blood coagulation proteins may profoundly alter their functions. When using liposomes or other model membranes, this parameter is typically not under experimental control.

I approached this problem by using a unique system of stable nanoscale phospholipid bilayers referred to as Nanodiscs as a platform for studying membrane-protein interactions [3]. Water-soluble Nanodiscs are produced by a self-assembly process resulting in a submicroscopic lipid bilayer encircled and stabilized by two copies of an amphipathic helical protein known as membrane scaffold protein (MSP). MSPs have been systematically elongated or truncated to yield stabilized, monodisperse phospholipid bilayers ranging from about 8 to 15 nm in diameter [4]. This self-assembly process is reproducible and efficient, yielding homogeneous preparations of supported lipid bilayers that are extremely stable and exhibit lipid fluidity comparable to liposomes [5,6]. Moreover, heterologous membrane-spanning proteins can also be incorporated efficiently into these supported nanobilayers [7,8]. Unlike liposomes and most other model membrane systems, the phospholipid bilayers in Nanodiscs cannot undergo long-range Ca^{2+}-induced reorganization of PS into regions of locally high PS content, which allows us to define the membrane composition immediately under and surrounding procoagulant proteins.

The assembly and characterization of 7.7 nm-diameter bilayer Nanodiscs containing net-neutral phospholipids have been firmly established by Stephen Sligar and his laboratory [9-12]. However, because blood clotting reactions occur preferentially in the presence of anionic phospholipids, bilayers containing just net neutral phospholipids are not ideal for the study of procoagulant proteins. Therefore, before conducting detailed studies with these proteins on Nanodiscs, it was necessary to assemble and characterize Nanodiscs containing PS in their membranes. Another consideration is that blood coagulation is initiated by TF, an integral membrane protein that functions optimally when embedded within a bilayer containing PS. As such, it was also necessary to integrate TF within a Nanodisc bilayer enriched with PS. This chapter therefore focuses on defining the Nanodisc system: its assembly, bilayer composition and aggregation state in the presence of physiological concentrations of Ca^{2+}. Finally, this chapter will also discuss the incorporation and characterization of active TF within the Nanodisc system.

2.2 EXPERIMENTAL PROCEDURES

2.2.1 Materials

PC (1-palmitoyl-2-oleoyl-*sn*-glycero-3-phosphocholine), PS (1-palmitoyl-2-oleoyl-*sn*-glycero-3-phosphoserine) and the lipid extruder were from Avanti Polar Lipids (Alabaster, AL). The molecular weights of PC and PS are 760 and 784 Da. Recombinant human TF, sTF and Nanodisc membrane scaffold proteins, MSP1D1 and MSP1E3D1 were expressed in *Esherichia coli* and purified as

previously described [13-15]. The molecular weights of MSP1D1 and MSP1D1E3 are 24.7 kD and 32.6 kDa respectively.

2.2.2 Preparation of Liposomes Containing Phosphatidylserine

Liposomes of varying PS content (with the balance being PC) were prepared by membrane extrusion. Briefly, mixtures of PC and PS (PCPS) in chloroform were dried under nitrogen and placed under vacuum to ensure complete solvent removal. The lipids were resuspended in TBS (50 mM Tris-HCl, 150 mM NaCl, 0.01% NaN_3, pH 7.4), subjected to 10 freeze-thaw cycles, and then extruded at least 10 times through two track-etched polycarbonate membranes (100 nm pores) using a double-syringe lipid extruder. This technique produces unilamellar vesicles with a mean diameter of approximately 80 nm [16]. Considering that the surface area of a PC headgroup is 0.7 nm^2 [17], an 80 nm-diameter liposome is calculated to comprise roughly 22,500 phospholipid molecules per leaflet.

2.2.3 Preparation of Nanodiscs Containing Phosphatidylserine

Nanodiscs containing 7.7 nm-diameter bilayers of varying PCPS content were prepared using sodium deoxycholate as the detergent. Briefly, PC and PS (5.2 mM total phospholipid) were dissolved in 10.4 mM sodium deoxycholate in TBS, after which MSP and TF were added to yield phospholipid:MSP molar ratios ranging from 65:1 to 70:1. Deoxycholate was subsequently removed using adsorbent polystyrene beads (Bio-Beads® SM-2; Bio-Rad, Hercules, CA), and

the resulting self-assembled Nanodiscs were purified using a Superdex 200 HR 30/10 size exclusion chromatography column as previously described [18]. Final ratios of phospholipid to MSP were quantified through a combination of inorganic phosphorus analysis for phospholipid [19,20] and A_{280} for MSP1D1, using an extinction coefficient of 21,000 M^{-1} cm^{-1}. To assess Nanodisc PCPS composition, the phospholipid content of purified 7.7 nm-diameter Nanodisc preparations were quantified by incorporating traces of ^{3}H-PS during self-assembly. Scintillation counting and the total phospholipid content by inorganic phosphate analyses following complete oxidation was used to determine PS recovery.

Nanodiscs containing 10.8 nm-diameter bilayers were prepared similarly, except MSP1E3D1, a larger variant of MSP1D1, was used [4]. Briefly, deoxycholate-solubilized mixtures of PCPS and MSP1E3D1 protein were prepared at a 120:1 molar ratio of phospholipid to MSP1E3D1. Deoxycholate was subsequently removed using Bio-Beads® SM-2, and the resulting self-assembled Nanodiscs were purified using size exclusion chromatography as before [18]. Final ratios of phospholipid to MSP were quantified through a combination of inorganic phosphorus analysis for phospholipid [19,20] and A_{280} for MSP1E3D1 using an extinction coefficient of 29,400 M^{-1} cm^{-1}.

2.2.4 Reconstitution of Tissue Factor into Liposomes and Nanodiscs

TF was incorporated into liposomes (TF-liposomes) as described [21], using sodium deoxycholate as the detergent. Briefly, mixtures of PC and PS in

chloroform were dried under nitrogen and placed under vacuum to ensure complete solvent removal. The lipids and TF were resuspended in 15 mM deoxycholate in TBS. Detergent was removed using Bio-Beads® SM-2. This produces a solution of relipidated TF with a molar ratio of phospholipid:TF of approximately 8,700:1.

TF was introduced into Nanodiscs as described for the incorporation of β_2-adrenergic receptors into Nanodiscs [7] with the following modifications: Mixtures of PC and PS (5.2 mM total phospholipid) were dissolved in 10.4 mM sodium deoxycholate in TBS, after which MSP and TF were added to yield phospholipid:MSP molar ratios ranging from 65:1 to 70:1, and MSP:TF molar ratios of 20:1. Detergent was removed using Bio-Beads® SM-2 and self-assembled Nanodiscs were isolated using size exclusion chromatography. Each Nanodisc contains two MSP proteins, this large excess of MSP to TF results in an average of one TF molecule per 10 Nanodiscs. This was done in order to minimize the occurrence of more than one TF molecule per Nanodisc.

2.2.5 Assessment of Nanodisc Aggregation in the Presence of Calcium Ions

Nanodiscs containing 0 to 100% PS were diluted in TBS with or without 2.5 mM $CaCl_2$ and incubated for a minimum of 20 min. This process was also performed on TF-Nanodiscs containing 75% PS. The samples were then resolved by size exclusion chromatography on a Superdex 200 column monitored by A_{280}. Nanodiscs with 7.7 nm-diameter bilayers were also analyzed

by dynamic light scattering in which intensity autocorrelation functions of micromolar quantities of TF-free Nanodiscs in TBS with or without 2.5 mM $CaCl_2$ were quantified at ambient temperature using a Brookhaven Instruments BI-200 SM goniometer with a Lexel model 95 argon-ion laser (514 nm) at a scattering angle of 90°. A photomultiplier tube was used to measure light intensity, with signal processing by a BI-9000AT digital correlator. Using the Siegert relationship, the intermediate scattering function, g, was determined from the measured intensity autocorrelation function, $G(\tau) = B(1 + f^2[g(\tau)]^2)$, where B is the background intensity, f is an optical constant based on the measuring instrument, and τ is the decay time [22].

2.2.6 Assessment of Tissue Factor Content and Function within Nanodiscs

Total TF concentrations in liposomes and Nanodiscs were determined by ELISA after detergent solubilization [21]. Concentrations of functional (available) TF in TF-liposomes and TF-Nanodiscs were determined enzymatically by titration with a fixed concentration of fVIIa [23]. With TF-Nanodiscs, TF concentrations measured by ELISA agreed with the results of fVIIa titrations within experimental error (not shown), indicating that essentially 100% of the TF molecules in TF-Nanodiscs were functional. With TF-liposomes, approximately 50 to 60% of the TF molecules measured by ELISA were available by fVIIa titration (not shown), attributable to some TF molecules facing the lumen of the liposomes. TF concentrations are given throughout as the concentration of available TF.

The TF-Nanodisc assembly process described above produces a mixture of Nanodiscs: a species containing TF (TF-Nanodiscs), and a species without TF (TF-free Nanodiscs). To demonstrate the presence of only one TF molecule per TF-Nanodisc, TF-Nanodiscs preparations were first purified from TF-free Nanodiscs by affinity chromatography using immobilized HPC4 antibody directed against an epitope tag at the N-terminus of TF, as previously described [13,24], but omitting the 1M NaCl wash step. These enriched TF-Nanodiscs were reanalyzed with a size-exclusion column monitored by A_{280} to verify their stability and size. Finally, the stoichiometries of TF and MSP in preparations of these enriched TF-Nanodiscs were then assessed via quantitative SDS PAGE.

To determine if TF incorporated in Nanodiscs retained cofactor function, the ability of TF-Nanodiscs of varying PS composition (from 20 to 100 mol%) to accelerate the clotting of plasma was investigated. The total phospholipid concentration was held constant at 50 μM and clot times were measured as a function of TF concentration. Similarly, the clot times of TF-Nanodiscs were also compared with TF-liposomes and soluble TF (sTF), two commonly used preparations of TF. For these preparations, the total phospholipid concentration was fixed at 50 μM using vesicles composed of 20% PS. The relative abilities of these TF preparations to induce blood coagulation was determined through a standard prothrombin time (PT) clotting assay using a STart® 4 coagulometer (Diagnostica Stago, Parsippany, NJ) according to the manufacturer's instructions. Briefly, these TF preparations at fixed TF concentrations were added to citrated

pooled normal plasma. Citrate inhibits blood coagulation due to its chelating

properties, and an excess of calcium chloride was used to initiate clotting and the

time of clot formation was measured. These measurements were all performed

at 37° C.

2.3   RESULTS AND DISCUSSION

2.3.1 The Phospholipid Composition of Nanodiscs can be Rigorously Controlled

Nanodiscs and TF-Nanodiscs containing 7.7 nm-diameter bilayers were

prepared using varying proportions of PC and PS, ranging from 0 to 100% PS.

These Nanodisc preparations were monodisperse, contained a mean of 67 ± 1

phospholipid molecules per leaflet and had final proportions of PC and PS that

faithfully reflected the input PC/PS content (Fig. 2.1). Likewise, Nanodiscs with

10.8 nm-diameter bilayers were found to contain a mean of 120 ± 4 phospholipid

molecules per leaflet as assessed by inorganic phosphorus content (for

phospholipids) and A_{280} (for MSP; data not shown).

In order to test the hypothesis that locally high PS content enhances blood

coagulation protein function, we needed to prepare Nanodiscs containing very

high mol% PS. This can be highly problematic when preparing liposomes, since

exposing liposomes with very high PS content to plasma concentrations of Ca^{2+}

leads to their aggregation, fusion and/or collapse [25]. Accordingly, we

investigated the aggregation state of Nanodiscs containing 0 to 100% PS. In the

absence of Ca^{2+}, both size Nanodiscs – containing 0 to 100% PS – were

monodisperse as assessed by size exclusion chromatography or dynamic light

scattering. In buffered solutions containing 150 mM NaCl and 2.5 mM $CaCl_2$,

Nanodiscs with 7.7 nm-diameter bilayers containing 0 to 90 mol% PS were

monodisperse as assessed by dynamic light scattering (Fig. 2.2, *A* and *B*) and

gel filtration (not shown). On the other hand, only 7.7 nm-diameter bilayer

Nanodiscs containing 100% PS showed limited but detectable aggregation in the

presence of Ca^{2+}, but not in its absence (Fig. 2.2*C*). Likewise, in the presence of

2.5 mM Ca^{2+}, we observed no detectable aggregation of Nanodiscs containing

10.8 nm-diameter bilayers composed of 0-70 mol% PS (Fig. 2.3, *A* and *B*). We

did observe some aggregation when these larger Nanodiscs contained 90% PS

(Fig. 2.3*C*). Our experiments with Nanodiscs containing 10.8 nm-diameter

bilayers in solution in the presence of calcium ions were therefore restricted to

Nanodiscs containing 0 to 70% PS.

2.3.2 Functional Tissue Factor can be Incorporated into Nanodiscs

During the assembly of 7.7 nm-diameter bilayer TF-Nanodiscs, a twenty-

fold excess of MSP1D1 to TF was used in order to ensure that no more than one

TF molecule inserted per Nanodisc. This however, produced a mixture of

Nanodiscs: a species with TF inserted (TF-Nanodiscs) and a species without TF

(TF-free Nanodiscs). For certain experiments, TF-Nanodiscs have been

separated from TF-free Nanodiscs through immunoaffinity chromatography

specific for an HPC4 affinity tag on the N-terminus of TF [13]. The HPC4

antibody binds to this peptide epitope in a Ca^{2+}-dependent manner and with very

34

high affinity, which allows for gentle elution of the tagged protein using EDTA. The presence of this epitope tag has no effect on TF procoagulant activity. Through this process, an enriched population of TF-Nanodiscs can be isolated. When reanalyzed on size-exclusion chromatography, these enriched TF-Nanodiscs elute with a more symmetrical peak and with a Stokes diameter that is slightly larger than TF-free Nanodiscs (Fig. 2.4).

The TF and MSP content of this enriched TF-Nanodisc preparation was also investigated via SDS-PAGE followed by Coomassie staining and densitometry (Fig. 2.5). Analysis of the SDS-treated TF-Nanodisc fraction shows both MSP and TF running in the same lane. When the densities of the bands are compared against known quantities of TF and MSP loaded on the same gel, a determination of 0.51 TF per MSP molecule was made. Since Nanodiscs have 2 MSP molecules, this corresponds to 1.02 TF molecules per TF-Nanodisc.

To determine if TF in Nanodiscs remained functional, the ability of TF-Nanodiscs of varying PS content to accelerate the clotting time of plasma was evaluated as a function of TF concentration (Fig. 2.6). Analysis of a standard PT clotting test demonstrated that TF-Nanodiscs do indeed possess appreciable procoagulant activity, with the fastest clotting times occurring at 20% PS.

The ability of TF-Nanodiscs to accelerate the coagulation of plasma was also judged against more conventional TF preparations. Using a standard PT clotting test, the clotting times of TF-Nanodiscs were compared with TF-liposomes and a mixture of sTF plus phospholipid vesicles as a function of TF

concentration (Fig. 2.7). These TF preparations had a total phospholipid concentration of 50 μM, composed of 20% PS. Results indicate that TF-Nanodiscs have a procoagulant activity that is somewhat less pronounced when compared to TF-liposomes but considerably more pronounced when compared to sTF. The slower clotting time of sTF underscores the importance of having a proper phospholipid membrane in the immediate vicinity of the TF molecule.

It is of note that the PT clotting assay used in this experiment is reliant upon two membrane-bound protease·cofactor pairs of the blood coagulation cascade: TF·VIIa and Va·Xa. Blood coagulation is initiated by TF·VIIa and the procoagulant activity induced by TF embedded in Nanodiscs indicates that the enzymatic ability of the TF·VIIa complex functions upon a 7.7 nm-diameter Nanodisc bilayer. However, because of the presence of excess phospholipids, this assay cannot adequately address if the Va·Xa complex functions on the Nanodisc surface. Understanding these events, therefore, require more detailed experiments and are discussed in the subsequent chapters.

2.3.3 The Nanodisc System Allows Rigorous Control of the Local Membrane Nanoenvironment

I have successfully produced nanometer-scale bilayers of defined size and PCPS compositions. Nanodiscs with 7.7 nm-diameter bilayers were found to contain a mean of 67 ± 1 phospholipid molecules per leaflet and had final proportions of PC and PS that were faithfully preserved throughout the assembly process. Likewise, Nanodiscs with 10.8 nm-diameter bilayers were found to

contain a mean of 120 ± 4 phospholipid molecules per leaflet. Except for

extreme circumstances, Nanodisc species containing PCPS bilayers are stable in

physiological amounts of Ca^{2+}. Moreover, active membrane-bound TF has been

successfully reconstituted into 7.7 nm-diameter Nanodiscs. These TF-Nanodiscs

have a stoichiometry of 1.02 TF molecules per Nanodisc and exhibit appreciable

procoagulant activity. Overall, these results demonstrate the viability of the claim

that these bilayers can be used as tightly-controlled membrane surfaces upon

which to control, assemble and study the components of the blood coagulation

cascade at the nanoscale level.

2.4   FIGURES
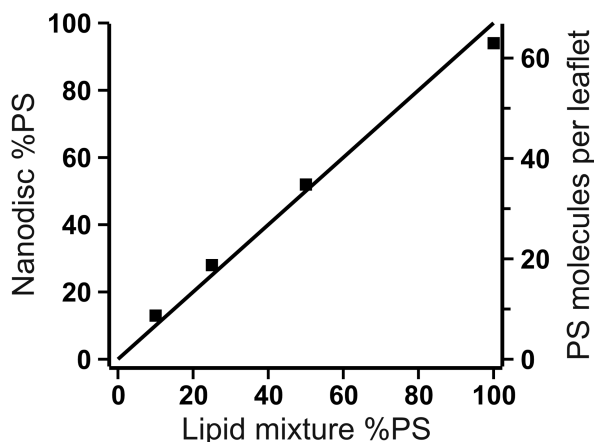
Figure 2.1   PS composition of Nanodiscs. PS content of Nanodiscs with 7.7
nm-diameter bilayers. Nanodiscs of varying PS compositions were prepared, to
which trace amounts of ^{3}H-PS were added during self-assembly. Scintillation
counting was used to determine PS recovery. The *line* is a plot of *y = x,* showing
that the %PS in Nanodiscs is essentially identical to that of the initial lipid mixture.
Inorganic phosphate analyses following complete oxidation of the samples
demonstrated that the mean molar ratio of phospholipid to MSP was 67(±1):1.
Since each Nanodisc contains two MSP molecules, the mean phospholipid
content was therefore 134 ± 2 phospholipid molecules per Nanodisc.

37
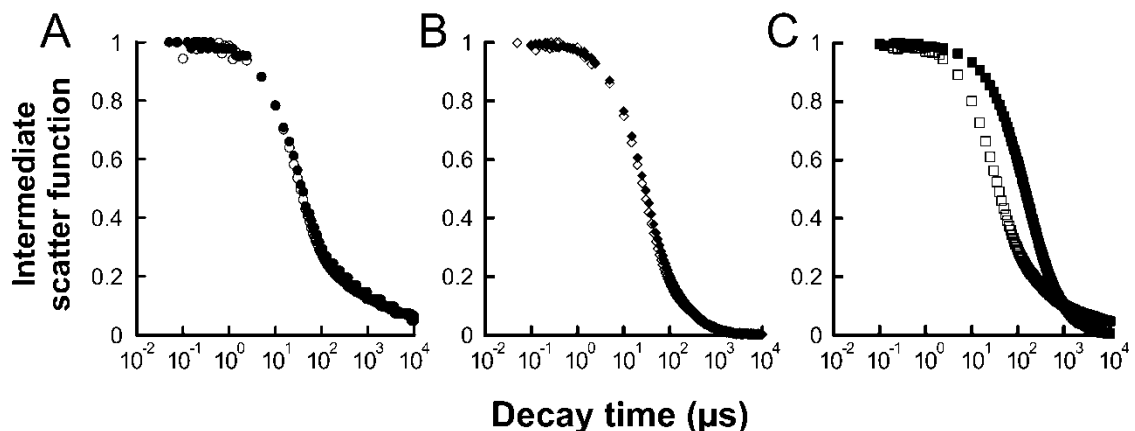
Figure 2.2   Intermediate scattering functions for 7.7 nm-diameter bilayer Nanodiscs of varying PS content. Dynamic light scattering for solutions of Nanodiscs with three representative PS compositions are shown: *A*, 0%; *B*, 90%; or *C*, 100% PS, analyzed in the presence (solid symbols) or absence (open symbols) of 2.5 mM $CaCl_2$. The coincidence of the curves $\pm$ Ca^{2+} (when the Nanodiscs contained from 0 to 90% PS, as seen in panels *A* and *B*) indicates lack of detectable aggregation induced by Ca^{2+}. Dynamic light scattering analyses of Nanodiscs with contents between 0 and 90% PS likewise exhibited no evidence of aggregation (not shown). Some evidence of aggregation was observed, however, when the Nanodiscs contained 100% PS, as evidenced by the shifted curve in the presence of Ca^{2+} (panel *C*).
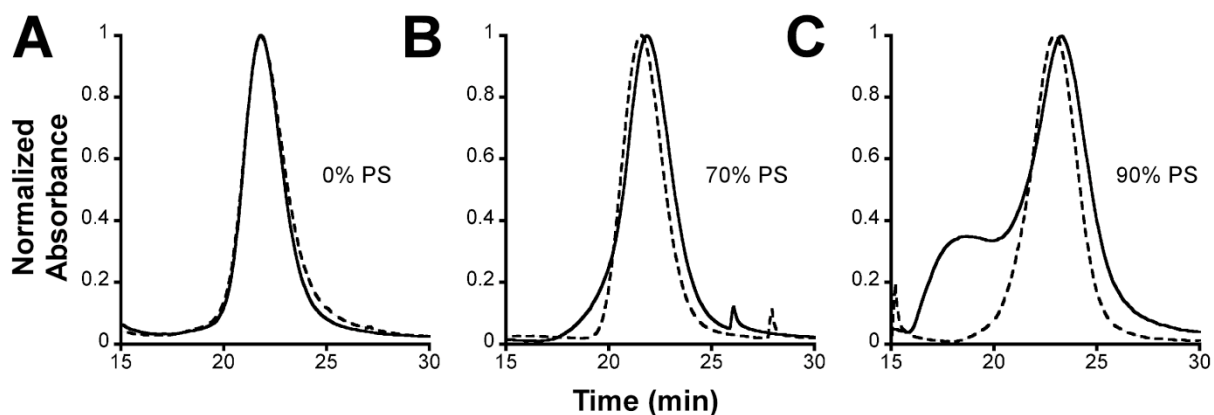
Figure 2.3   Size exclusion chromatographs for 10.8 nm diameter bilayer Nanodiscs of varying PS content. Normalized size exclusion chromatographs for solutions of Nanodiscs of three representative PS compositions are shown: *A*, 0%; *B*, 70%; or *C*, 90% PS, analyzed in the presence (*solid lines*) or absence (*dotted lines*) of 2.5 mM $CaCl_2$. Coincidence of curves in *A* and *B* in the presence of absence of Ca^{2+} indicate lack of detectable aggregation. Size exclusion chromatography of Nanodiscs with contents between 0 and 70% PS, likewise, exhibited no evidence of aggregation (not shown). Some evidence of aggregation was observed, however, when Nanodiscs contained 90% PS, as evidenced by the shouldering at ~18 min in the presence of Ca^{2+}.
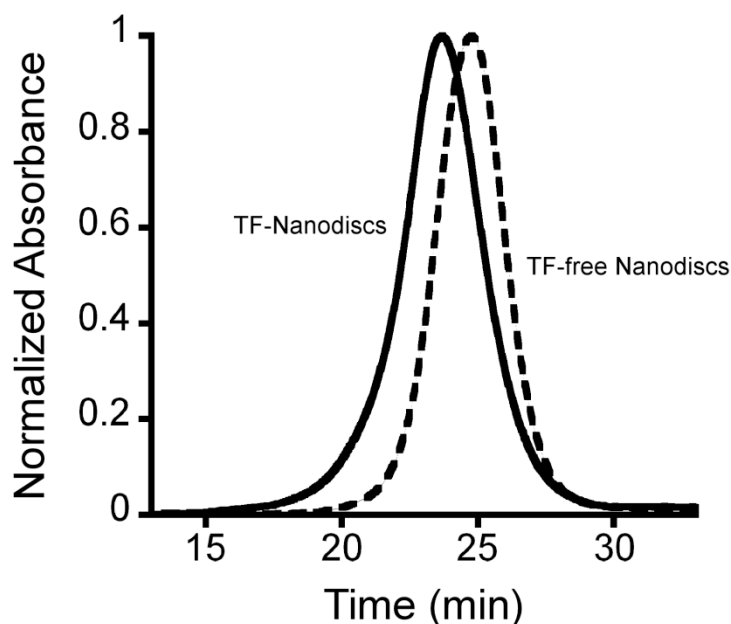
Figure 2.4   Representative gel filtration chromatographs of 7.7 nm-diameter bilayer Nanodisc preparations.   Normalized size exclusion chromatographs for TF-free Nanodiscs (*dotted lines*) and enriched TF-Nanodiscs (*solid lines*). Comparison of curves indicates a faster elution time for TF-Nanodiscs, corresponding to a slightly larger Stokes diameter than TF-free Nanodiscs. These samples contained 75% PS (with the balance being PC) and were loaded sequentially on an equilibriated size-exclusion column monitored at A_{280}.
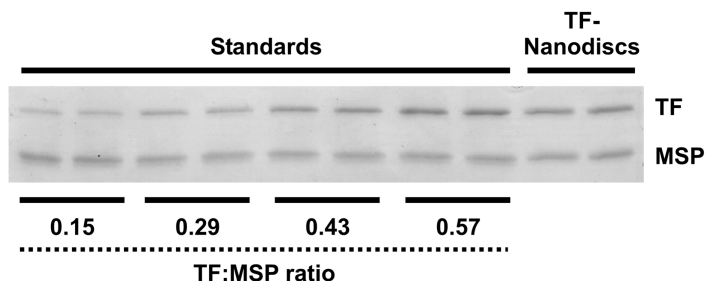
Figure 2.5   Number of tissue factor molecules per Nanodisc. A standard curve was prepared by resolving samples, in duplicate, containing known quantities of purified TF and MSP (*first eight lanes*) on SDS-PAGE, staining the gel with Coomassie Blue and digitizing using a scanning densitometer (analyzed using Scion Image software, Scion Corporation, Frederick, MD). Purified TF-Nanodiscs were resolved on the same gel (*rightmost two lanes*) and quantified in parallel with the standards, yielding a determination of 0.51 TF/MSP molecule, or 1.02 TF molecules/TF-Nanodisc.

40
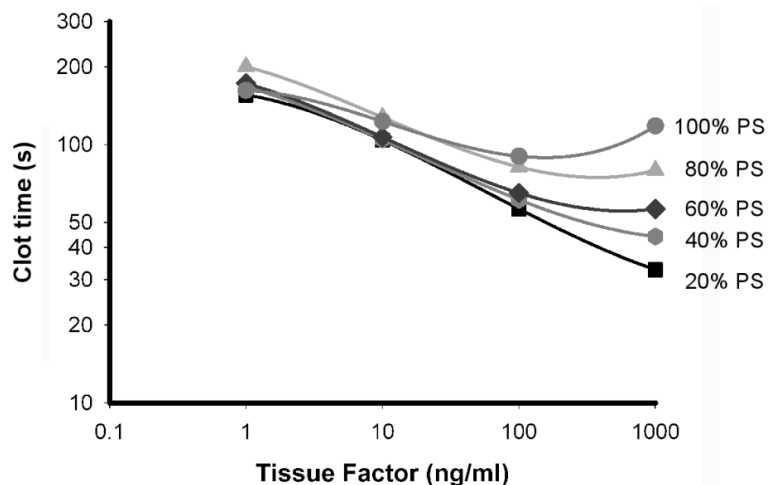
Figure 2.6   Clotting activity of TF-Nanodiscs containing varying PS content. The ability of TF-Nanodiscs of varying PS content (from 20 to 100 mol%) to shorten the clotting time of plasma was assayed via a standard prothrombin time test as a function of TF concentration. Total phospholipid concentration was held constant at 50 μM.
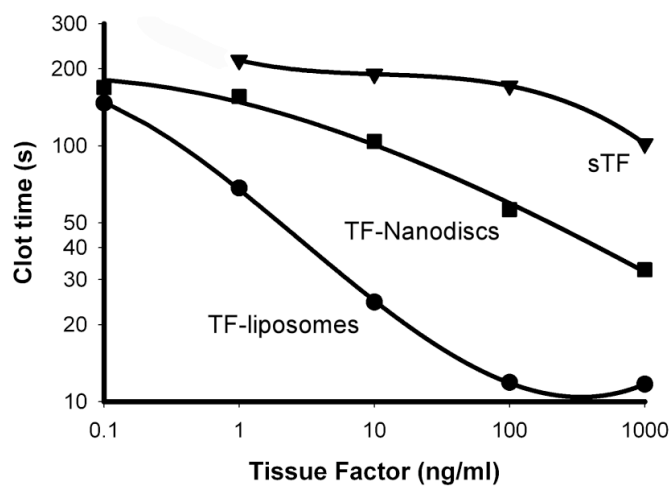
Figure 2.7   Clotting activity of three tissue factor preparations. TF-induced clot times were measured for tissue factor relipidated into Nanodiscs (TF-Nanodiscs), tissue factor relipidated into liposomes (TF-liposomes), and a mixture of soluble tissue factor (sTF) plus PCPS vesicles. Tissue factor concentration was varied and total phospholipid concentration was held constant at 50 μM and at 20% PS for all preparations. sTF concentrations below 1 ng/ml produced clot times of > 300 s.

41

2.5 REFERENCES

1. Haverstick DM, Glaser M. Visualization of Ca2+-induced phospholipid domains. *Proc Natl Acad Sci U S A* 1987; **84:** 4475-4479.

2. Yang L, Glaser M. Formation of membrane domains during the activation of protein kinase C. *Biochemistry* 1996; **35:** 13966-13974.

3. Bayburt TH, Grinkova YV, Sligar SG. Self-assembly of discoidal phospholipid bilayer nanoparticles with membrane scaffold proteins. *Nano Lett* 2002; **2:** 853-856.

4. Denisov IG, Grinkova YV, Lazarides AA, Sligar SG. Directed self-assembly of monodisperse phospholipid bilayer Nanodiscs with controlled size. *J Am Chem Soc* 2004; **126:** 3477-3487.

5. Shaw AW, McLean MA, Sligar SG. Phospholipid phase transitions in homogeneous nanometer scale bilayer discs. *FEBS Lett* 2004; **556:** 260-264.

6. Denisov IG, McLean MA, Shaw AW, Grinkova YV, Sligar SG. Thermotropic phase transition in soluble nanoscale lipid bilayers. *J Phys Chem B Condens Matter Mater Surf Interfaces Biophys* 2005; **109:** 15580-15588.

7. Leitz AJ, Bayburt TH, Barnakov AN, Springer BA, Sligar SG. Functional reconstitution of Beta2-adrenergic receptors utilizing self-assembling Nanodisc technology. *BioTechniques* 2006; **40:** 601-2, 604, 606, passim.

8. Bayburt TH, Sligar SG. Self-assembly of single integral membrane proteins into soluble nanoscale phospholipid bilayers. *Protein Sci* 2003; **12:** 2476-2481.

9. Civjan NR, Bayburt TH, Schuler MA, Sligar SG. Direct solubilization of heterologously expressed membrane proteins by incorporation into nanoscale lipid bilayers. *Biotechniques* 2003; **35:** 556-3.

10. Denisov IG, Grinkova YV, Lazarides AA, Sligar SG. Directed self-assembly of monodisperse phospholipid bilayer Nanodiscs with controlled size. *J Am Chem Soc* 2004; **126:** 3477-3487.

11. Baas BJ, Denisov IG, Sligar SG. Homotropic cooperativity of monomeric cytochrome P450 3A4 in a nanoscale native bilayer environment. *Arch Biochem Biophys* 2004; **430:** 218-228.

12. Duan H, Civjan NR, Sligar SG, Schuler MA. Co-incorporation of heterologously expressed Arabidopsis cytochrome P450 and P450 reductase into soluble nanoscale lipid bilayers. *Arch Biochem Biophys* 2004; **424:** 141-153.

13. Rezaie AR, Fiore MM, Neuenschwander PF, Esmon CT, Morrissey JH. Expression and purification of a soluble tissue factor fusion protein with an epitope for an unusual calcium-dependent antibody. *Protein Expr Purif* 1992; **3:** 453-460.

14. Smith SA, Morrissey JH. Rapid and efficient incorporation of tissue factor into liposomes. *J Thromb Haemost* 2004; **2:** 1155-1162.

15. Bayburt TH, Sligar SG. Single-molecule height measurements on microsomal cytochrome P450 in nanometer-scale phospholipid bilayer disks. *Proc Natl Acad Sci U S A* 2002; **99:** 6725-6730.

16. MacDonald RC, MacDonald RI, Menco BP, Takeshita K, Subbarao NK, Hu LR. Small-volume extrusion apparatus for preparation of large, unilamellar vesicles. *Biochim Biophys Acta* 1991; **1061:** 297-303.

17. Kucerka N, Tristram-Nagle S, Nagle JF. Structure of fully hydrated fluid phase lipid bilayers with monounsaturated chains. *J Membr Biol* 2005; **208:** 193-202.

18. Shaw AW, Pureza VS, Sligar SG, Morrissey JH. The local phospholipid environment modulates the activation of blood clotting. *J Biol Chem* 2007; **282:** 6556-6563.

19. Fiske C, SubbaRow Y. The Colorimetric Determination of Phosphorus. *J Biol Chem* 1925; **66:** 375-400.

20. Chen PS, Toribara TY, Warner H. Microdetermination of phosphorus. *Anal Chem* 1956; **28:** 1756-1758.

21. Smith SA, Morrissey JH. Rapid and efficient incorporation of tissue factor into liposomes. *J Thromb Haemost* 2004; **2:** 1155-1162.

22. *Dynamic Light Scattering: Applications of Photon Correlation Spectroscopy*. New York: Plenum Press, 1985.

23. Neuenschwander PF, Fiore MM, Morrissey JH. Factor VII autoactivation proceeds via interaction of distinct protease-cofactor and zymogen-cofactor complexes. Implications of a two-dimensional enzyme kinetic mechanism. *J Biol Chem* 1993; **268:** 21489-21492.

24. Rezaie AR, Fiore MM, Neuenschwander PF, Esmon CT, Morrissey JH. Expression and purification of a soluble tissue factor fusion protein with an epitope for an unusual calcium-dependent antibody. *Protein Expr Purif* 1992; **3:** 453-460.

25. Wilschut J, Duzgunes N, Hoekstra D, Papahadjopoulos D. Modulation of membrane fusion by membrane fluidity: temperature dependence of divalent cation induced fusion of phosphatidylserine vesicles. *Biochemistry* 1985; **24:** 8-14.

CHAPTER 3

THE LOCAL PHOSPHOLIPID ENVIRONMENT MODULATES THE ACTIVATION OF BLOOD CLOTTING

3.1   BACKGROUND

In both normal hemostasis and many life-threatening thrombotic diseases, blood clotting is triggered when tissue factor (TF), an integral membrane protein, binds the plasma serine protease, factor VIIa (fVIIa) [1]. The resulting two-subunit, membrane-bound enzyme, TF·VIIa, activates the plasma zymogens, factors IX (fIX) and X (fX), by limited proteolysis. Erwin Chargaff (of nucleic acids fame) demonstrated in the 1940s that TF procoagulant activity requires it to be associated with phospholipids, and research over the ensuing decades demonstrated that TF is a membrane-spanning protein that must be incorporated into bilayers containing anionic phospholipids for optimal activity (reviewed by Bach [2]). Despite this extensive history, we still have an indistinct picture of how anionic phospholipids contribute so profoundly to the enzymatic activity of membrane-bound protease complexes involved in blood clotting [3].

Membranes composed of mixed phospholipids (and other lipids) can form membrane microdomains with locally different surface properties. A noted example is the formation of cholesterol- and sphingolipid-rich lipid rafts and caveolae on cell surfaces [4,5]. Experiments using giant unilamellar vesicles have shown that even liposomes containing simple binary mixtures of neutral and anionic phospholipids spontaneously form anionic phospholipid-rich membrane

microdomains in the presence of plasma concentrations of Ca^{2+}, which is even more pronounced in the presence of membrane-binding proteins [6,7]. Thus, anionic phospholipids were shown to coalesce, via lateral diffusion over relatively large distances, into subdomains several μm in size. These and other studies have demonstrated that local membrane microenvironments can differ dramatically from the average composition of the membrane even in relatively "simple" model membranes.

Most clotting proteins bind reversibly and in a Ca^{2+}-dependent manner to bilayers containing anionic phospholipids—with phosphatidylserine (PS) being most active. Local differences in membrane microdomain properties mean that specific proteins may tend to partition into or out of such microdomains, and so the lipid composition in the immediate vicinity of membrane-bound protease-cofactor complexes may be expected to profoundly influence their enzymatic activities. For example, TF-bearing microparticles have been reported to arise from lipid rafts [8], and depletion of cholesterol from cell membranes impairs functional TF expression in fibroblasts [9]. TF has also been reported to associate with caveolae on some cell surfaces [10-12]. The mechanisms by which specific plasma membrane domains may regulate the rate of clotting reactions are largely unknown, however. Membrane-binding protein substrates such as fX are known to partition between the solution phase and the membrane surface, and most likely they also partition into specific membrane microdomains. We therefore hypothesize that blood clotting reactions such as the activation of

fX by the TF·VIIa complex occur preferentially, or at least with greatest efficiency, within membrane microdomains that have locally very high PS content.

fX molecules bound to the membrane may translate on the membrane via lateral diffusion, effectively skating or hopping along the surface. This leads to at least two different possible mechanisms by which protein substrates such as fX can encounter the TF·VIIa complex. In one mechanism, solution-phase fX binds directly to the membrane-bound TF·VIIa complex, whereupon it is activated to fXa via limited proteolysis. In another mechanism, membrane-bound fX molecules that are translating along the membrane surface (via lateral diffusion or hopping) encounter the TF·VIIa complex. Several studies have addressed the relative importance of these two modes of substrate delivery to the TF·VIIa complex, typically by incorporating TF into liposomes of defined phospholipid composition, assembling the TF·VIIa complex, and then quantifying rates of fX activation. These approaches have allowed somewhat indirect inferences to be made regarding the choice of solution-phase versus membrane-bound fX as the preferred substrate, in which the investigators systematically vary the liposome concentration and also use competing membrane-binding proteins. Using such approaches, some investigators have concluded that the membrane-bound pool of fX is the preferred substrate [13], while others have concluded the opposite— that solution-phase fX is the preferred substrate for the TF·VIIa complex [14,15].

In this study, we tested the concept that the local membrane nanoenvironment surrounding coagulation protease-cofactor complexes controls

both their assembly and catalytic efficiencies toward membrane-bound protein substrates. We approached this by incorporating TF into nanoscale phospholipid bilayers that allow rigorous control of the local membrane microenvironment. This was accomplished using a unique system of stable nanoscale phospholipid bilayers, termed Nanodiscs [16], as a platform for studying membrane-protein interactions. Water-soluble Nanodiscs are produced by a self-assembly process resulting in a nanoscale lipid bilayer (about 8 nm in diameter) encircled and stabilized by two copies of an amphipathic helical protein termed membrane scaffold protein (MSP). This self-assembly is reproducible and efficient, yielding monodisperse preparations of supported lipid bilayers that are extremely stable and that exhibit lipid fluidity comparable to liposomes [17,18]. Moreover, heterologous membrane-spanning proteins can also be incorporated efficiently into these supported nanobilayers during self-assembly [19,20]. By embedding TF into nanoscale lipid bilayers, we can preclude long-distance (μm scale) recruitment of PS molecules into membrane domains with locally high or low PS content. Instead, the composition of the membrane nanodomain *immediately* surrounding the TF·VIIa complex is under tight experimental control. Using this system, we report that full TF·VIIa proteolytic activity required extremely high local concentrations of anionic phospholipids, and furthermore that a large pool of membrane-bound fX was not required to support efficient catalysis.

3.2   EXPERIMENTAL PROCEDURES

3.2.1   Materials

Phosphatidylcholine (PC; 1-palmitoyl-2-oleoyl-*sn*-glycero-3-phosphocholine) and PS (1-palmitoyl-2-oleoyl-*sn*-glycero-3-phosphoserine) were from Avanti Polar Lipids (Alabaster, AL), fVIIa was from American Diagnostica (Greenwich, CT) and fX was from Enzyme Research Laboratories (South Bend, IN). Recombinant human TF [21] and MSP [16] were expressed in *E. coli* and purified as described.

3.2.2   Measuring the Binding of fVIIa to TF-Nanodiscs and Rates of fX Activation

Binding affinities of fVIIa for TF in liposomes or Nanodiscs were quantified using the TF-dependent increase in fVIIa enzymatic activity as described [22]. Initial rates of fX activation by the TF·VIIa complex (assembled either on TF-liposomes or TF-Nanodiscs) were quantified using a continuous fX activation assay as previously described [22]. Rates of fXa generation were measured over a 20 min period and in all cases were linear over the entire time course. In all kinetic experiments, the final TF concentration was 5 pM in both the TF-Nanodisc and TF-liposome systems. For TF-Nanodisc experiments, a molar ratio of 1 TF-Nanodisc: 9 TF-free Nanodiscs was used, yielding final concentrations of 50 pM Nanodiscs and 6.7 nM phospholipid. For TF-liposome experiments, the final phospholipid concentration was 65 nM. K_m and k_{cat} values were calculated by fitting the Michaelis-Menten equation to the rate data using nonlinear regression.

3.2.3 Surface Plasmon Resonance Analyses

Binding of fX to Nanodiscs containing varying mol% PS was quantified by surface plasmon resonance using a Biacore 3000 instrument. NTA Biacore sensor chips were charged with Ni^{2+} according to the manufacturer's recommendations, after which Nanodiscs were immobilized on the NTA-Ni^{2+} chip surface via the oligohistidine tag located on MSP. An empty NTA-Ni^{2+} channel was used to subtract changes in resonance units (RU) due to the refractive index of the protein solution and any non-specific binding. Running buffer (10 mM HEPES-NaOH pH 7.4, 150mM NaCl, 2.5mM $CaCl_2$) was flowed at $5\mu L$/min. Nanodiscs were loaded onto each channel in calcium-free running buffer until a signal of 800 RU was achieved, after which a steady baseline was established in running buffer. Increasing concentrations of fX were injected in running buffer and the maximal response above the baseline upon reaching steady state was recorded for each injected concentration. The maximal RU values achieved at each fX concentration were then used to evaluate the affinity (K_d) of fX for the nanoscale bilayers. This approach avoids potential limitations from analyzing association and dissociation rate data due to mass transport-limited rates of analyte association and analyte rebinding during the dissociation phase. At the end of each run, NTA chips were regenerated using a buffer containing 0.3 M EDTA, which successfully removed the Nanodiscs and all bound proteins. NTA sensor chips were reused for multiple binding experiments with no observed loss of function.

3.3   RESULTS AND DISCUSSION

In this study we examined how changes in the local composition of the membrane *immediately* surrounding the TF·VIIa complex modulated its ability to proteolytically activate its membrane-binding substrate, fX. We approached this by embedding TF into supported nanoscale lipid bilayers (Nanodiscs), in order to preclude long-distance recruitment of PS molecules into membrane subdomains with locally high or low PS contents. As presented below, we then measured the ability of the TF·VIIa complex to assemble and function within these nanoscale bilayers as the local PS content was altered over a very broad range (0 to 90% PS). In order to show the general trends observed with conventional liposome-based approaches, we obtained data with the TF·VIIa complex assembled on TF-liposomes of varying phospholipid composition (from 0 to 40% PS). For the reasons outlined in the Introduction, however, it is not really possible to compare directly the results obtained using these two forms of TF, since we have no experimental control over the local PS content surrounding the TF·VIIa complex assembled on TF-liposomes. Furthermore, because conventional liposomes containing extremely high PS contents undergo vesicle fusion and collapse when exposed to mM concentrations of Ca^{2+} [23], it is likewise not possible to study the effects of high total PS content in conventional TF-liposomes.

3.3.1 Size Considerations

In order to successfully investigate the activation of blood coagulation using the Nanodisc system, it was essential to demonstrate that the enclosed nanobilayer has sufficient room to assemble the TF·VIIa complex and also to productively bind at least one substrate (fX) molecule. The cross-sectional area of the membrane-binding domain of fVIIa (the Gla domain) is ~3.9 nm^2 [24], and the surface area of a phospholipid headgroup is ~0.7 nm^2 [25], so the Gla domain covers roughly six phospholipid molecules. The nanobilayers in these Nanodiscs, which contain 67±1 phospholipid molecules per leaflet (see below), should therefore have room to bind as many as ten Gla domains per leaflet. But the cross-sectional area of the widest part of the TF·VIIa complex—near the globular fVIIa protease domain—is 16 to 18 nm^2 [24], or enough to cover 23 to 26 phospholipid molecules. The relative sizes of these structures are displayed graphically in Fig. 3.1*A*, in which the crystal structure of the TF·VIIa complex is placed, to scale, on a schematic of the 8 nm supported bilayer contained within a Nanodisc. Although the widest part of the TF·VIIa complex is around the globular protease domain of fVIIa, the two points of membrane contact in the TF·VIIa complex are considerably smaller. Furthermore, since the supported bilayer in Nanodiscs has a boundary, portions of the TF·VIIa complex located near the protease domain could project beyond the edge of the bilayer. This is demonstrated graphically in Figs. 3.1*B* and *C*, in which a "top" view of the crystal structure of the TF·VIIa complex is placed, to scale, on an 8 nm diameter circle

representing the size of the supported nanobilayers [26]. In this case, over 60%

of the surface of the leaflet remains available for binding fX molecules. The

three-dimensional structure of zymogen fX is not known with certainty but fX is

highly homologous to fVII (including its Gla domain) and likely has a similar

cross-sectional area. With 60% or more of the disc surface still available on

discs containing the TF·VIIa complex, as many as six fX molecules could also

possibly bind to the remaining leaflet. However, factors such as the mobility of

TF·VIIa in the lipid bilayer and the need for fX to bind in a specific orientation

relative to TF·VIIa might reduce the available area somewhat. Thus, the lipid

bilayer in a Nanodisc is large enough to assemble the TF·VIIa complex and also

bind at least one fX molecule, and perhaps as many as five or six.

3.3.2 Binding of fX to Nanoscale Bilayers

Incorporating PS into TF-liposomes of mixed phospholipid content

enhances TF·VIIa proteolytic activity, with maximal rates of fX activation

generally achieved at 10 to 40% PS [27,28]. This rate enhancement requires the

presence of the Gla domain on fX, which mediates reversible binding of this

protein to membranes containing PS. Accordingly, we used surface plasmon

resonance to examine the ability of nanoscale bilayers of varying PS content to

bind fX. Fig. 3.2*A* shows plots of the maximal RU values obtained at steady state

for binding of fX to Nanodiscs of varying PS content, plotted as amount bound

versus fX concentration. Negligible quantities of fX bound to Nanodiscs

containing only PC, but as the PS content of the nanobilayers increased, fX was

observed to bind to Nanodiscs in a saturable, concentration-dependent manner in which both the affinity and total amount of fX binding increased with increasing PS content. The single-site ligand binding equation fit very well to the data at all PS contents (Fig. 3.2A), from which K_d values were obtained. Binding affinities increased (*i.e.*, K_d values decreased) as a function of increasing PS content (Fig. 3.2B), with an almost linear dependence of binding free energy on PS content (Fig. 3.2C). The K_d values obtained with Nanodiscs containing 54 or 67 PS molecules per leaflet (*i.e.,* 80 or 100% PS) were in the range of literature values for fX binding to liposomes containing 20 to 30% PS [29,30]. Interestingly, the amount of fX bound to Nanodiscs at saturation increased steadily as the PS content increased (Fig. 3.2D), and indeed previous studies using liposomes have estimated that one fX molecule engages approximately five PS molecules [29]. Thus, Nanodiscs with very high PS content will contain more fX binding sites, and as the PS molecules are more closely packed within the bilayer they will bind fX with higher affinity.

As demonstrated above, there is theoretically sufficient room on Nanodiscs to bind up to ten fX molecules per leaflet. Stoichiometric calculations of fX molecules bound per Nanodisc can be estimated from SPR signals if the bound molecules have equivalent impact on the refractive index. Previous studies have shown that phospholipid bilayers in the fluid phase have similar refractive indices compared with protein solutions [31,32]. Therefore, at saturation the molar ratio of fX to Nanodiscs equals

$(RU_{fX}/RU_{discs})*(MW_{discs}/MW_{fX})$. In our experiments, 800 RU of Nanodiscs were loaded onto the sensor chips. The maximal amount of fX bound at steady state increased linearly as a function of the PS content of the Nanodiscs, with 5100 RU of fX bound at saturation to discs containing 100% PS. Using masses of 154 kDa for Nanodiscs containing 100% PS (*i.e.*, 134 PS molecules at 784 Da each and 2 MSP molecules at 24.7 kDa each) and 59 kDa for fX, we calculated 16.6 fX molecules bound per Nanodisc (*i.e.*, 8.4 fX bound per leaflet) at saturation (Fig. 3.2*D*). This agrees well with the maximal estimate of about ten fX molecules per leaflet based solely on the surface area of a Gla domain. Using 0.7 nm^2/phospholipid, this corresponds to a surface coverage of 29 pmol fX/cm^2, which is significantly higher than reported in the literature in experiments using fX binding to liposomes [30,33]. We attribute this apparently higher coverage to the fact that Nanodiscs have boundaries beyond which the globular portions of these proteins can project (as demonstrated graphically by the TF·VIIa complex in Fig. 3.1), and also to the very high local PS content of these Nanodiscs (leading to a higher density of potential fX binding sites).

3.3.3 Assembling the TF·VIIa Complex on Nanoscale Bilayers

Most of the binding energy of the TF·VIIa complex comes from protein-protein interactions, but some additional binding energy is provided by protein-membrane interactions between the fVIIa Gla domain and anionic phospholipids, thereby reducing the K_d for assembling TF·VIIa from ~2 nM to less than 50 pM [27]. In the present study we found that binding of fVIIa to TF in liposomes or

55

Nanodiscs was enhanced as the PS content of the bilayer increased, achieving K_d values below 30 pM for both presentations of TF (Fig. 3.3). Interestingly, the tightest binding of fVIIa to TF-Nanodiscs was observed at the highest PS contents (70 and 90% PS). This is consistent with the notion that locally very high PS content favors the binding of Gla domain-containing proteins such as fVIIa to membrane surfaces. This also suggests that the TF·VIIa complex will have highest affinity for, and therefore likely to partition into, membrane subdomains with locally very high PS content. Our findings also demonstrate that it is possible to assemble fully functional TF·VIIa complexes on 8 nm diameter bilayers.

3.3.4 Local PS Composition Influences Rates of fX Activation by TF·VIIa

As expected from many previous studies, increasing the PS content of TF-liposomes decreased the apparent K_m for fX activation by TF·VIIa (Fig. 3.4A). With TF-Nanodiscs, the K_m for fX decreased monotonically as the PS content increased (Fig. 3.4B), paralleling the PS dependence of fX binding to Nanodiscs (cf. Fig. 3.2B). Interestingly, the lowest K_m values with TF-Nanodiscs were obtained at the highest PS content (containing 60 PS molecules per leaflet, or 90% PS). It should also be noted that these kinetic experiments employ 50 pM Nanodiscs, each of which can bind a maximum of about 16.6 fX molecules. Thus, the *maximal* concentration of membrane-bound fX is about 0.8 nM, which is far below the fX concentrations used in our kinetic analyses. For this reason,

the concentration of total fX and free fX are essentially identical in our kinetic studies using TF-Nanodiscs.

We obtained similar apparent k_{cat} values when TF·VIIa complex was assembled on TF-Nanodiscs and TF-liposomes, ranging from about 1 to 4 s^{-1} (Fig. 3.4C), although the trends in k_{cat} values differed somewhat between TF-liposomes and TF-Nanodiscs as the PS content increased. With TF-liposomes the second-order rate constant for fX activation (k_{cat}/K_m) increased continuously with increasing %PS from 10 to 40% PS, and with TF-Nanodiscs it increased from 10 to 70% PS (equivalent to 47 PS molecules per leaflet). Taken together, these results indicate that the TF·VIIa complex is most active when the local PS content is very high (70% PS and above).

3.3.5 Mechanisms of Substrate Presentation to TF·VIIa

Our findings demonstrate that the TF·VIIa enzyme complex can efficiently activate its natural protein substrate, fX, even when this membrane-bound enzyme complex is constrained within a nanoscale lipid bilayer consisting of only ~67 phospholipid molecules per leaflet. From indirect analyses using TF-liposomes, some have suggested that solution-phase fX may be the preferred substrate for TF·VIIa [14,15], while others have argued that the pool of membrane-bound fX represents the preferred substrate [13]. The TF·VIIa complex assembled on Nanodiscs, unlike the situation on liposomes, does not have access to a large pool of membrane-bound fX molecules that can be used to deliver substrate to the enzyme over long distances by lateral diffusion or

hopping. Instead, the tiny membrane surface corralled inside the Nanodisc can

bind at most five or six fX molecules when the TF·VIIa complex is present, as

discussed above. Given the rates of fX activation observed in Fig. 3.4, it should

take only two or three seconds to convert all these membrane-bound fX

molecules to fXa. Instead, we observed linear rates of fX activation that were

sustained over 20 min. At a k_{cat} of 2 s^{-1}, each TF·VIIa complex activates 2400 fX

molecules during this 20 min time course. Therefore, the TF·VIIa complex must

rely on continuous binding of substrate (fX) to, and dissociation of product (fXa)

from the nanobilayer, in order to allow such sustained rates of fX activation. On

the other hand, the much larger membrane surface on liposomes can bind many

hundreds of fX molecules, theoretically allowing the TF·VIIa complex to choose

between the membrane-bound pool of fX molecules laterally diffusing on the

membrane surface or solution-phase fX molecules that bind directly to TF·VIIa or

to the membrane immediately adjacent to complex. The fact that k_{cat} values

obtained with TF-Nanodiscs rival those of TF-liposomes indicates that the

TF·VIIa complex is not absolutely dependent on a large, preexisting pool of

membrane-bound fX to serve as substrate.

 With TF-liposomes, k_{cat} values increased as the %PS increased (up to

40% PS), but TF-Nanodiscs did not exhibit this behavior. Hathcock *et al.*, [30,34]

proposed that removal of fXa from the vicinity of the TF·VIIa complex by lateral

diffusion on the membrane surface is likely the rate-limiting process controlling

the apparent k_{cat}. However, this mechanism of product removal from the TF·VIIa

complex is likely to be less effective when the TF·VIIa complex is constrained within nanoscale bilayers.

Coagulation serine proteases and the corresponding protease-cofactor complexes (including TF·VIIa) have evolved exosites to increase substrate specificity [35]. Exosites are distinct binding sites lying outside the protease's active site that can enhance binding of protein substrates, inhibitors and other regulatory molecules. In fact, exosites may be located on the protease, the protein cofactor, or both. We propose that a small patch of anionic phospholipids located on the membrane surface in the immediate vicinity (*i.e.*, within a few nm) of TF serves as an additional exosite to enhance the binding affinity of protein substrates like fIX and fX to the TF·VIIa complex. This contributes in an important way to the substrate specificity of this extremely selective activator of the blood clotting cascade.
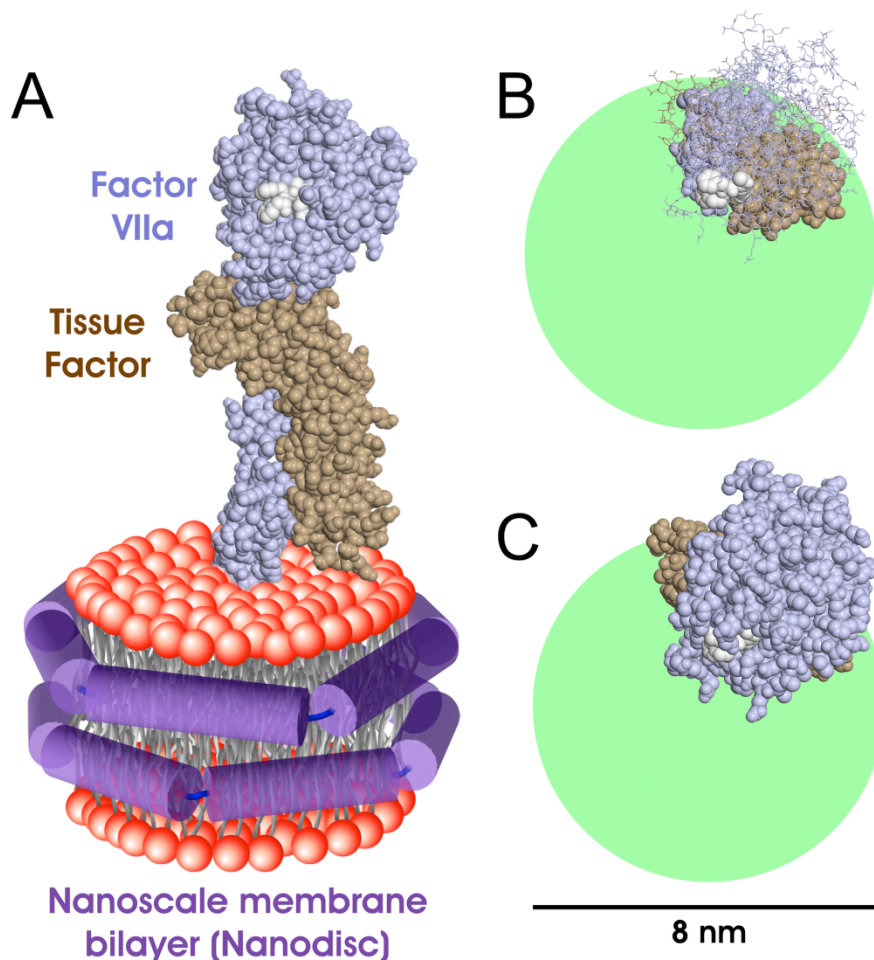
Figure 3.1   Schematic of the TF·VIIa complex on an 8 nm supported nanoscale bilayer. *A*, The TF·VIIa crystal structure (PDB file 1DAN [24]) is placed, to scale, on a schematic of the 8 nm diameter bilayer in a Nanodisc [16]. TF is colored brown, fVIIa is blue (with active site inhibitor in white), phospholipid headgroups are depicted as red spheres, and amphipathic helices of the encircling MSP are depicted as purple cylinders. *B*, "Top" view of the TF·VIIa complex placed near the edge of an 8 nm diameter bilayer (represented by a green circle), with only the Gla domain of fVIIa and the "bottom" portion of TF rendered as space filling atoms; the rest of the TF·VIIa structure (except the active site inhibitor) is rendered as wires. *C*, Same view as in panel *B*, but with the entire TF·VIIa complex rendered as space-filling atoms.
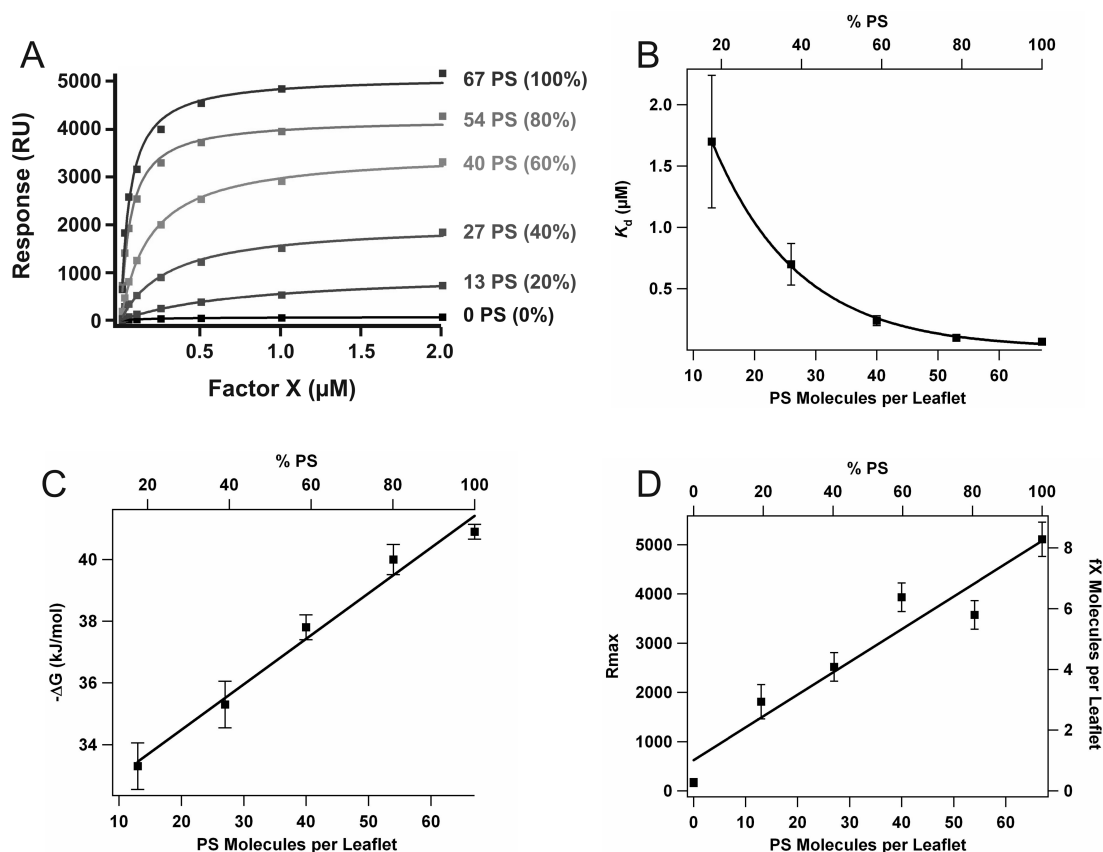
Figure 3.2   Binding of fX to Nanodiscs of varying PS content, measured by surface plasmon resonance. *A*, Steady-state binding of fX to Nanodiscs with the indicated number of PS molecules per leaflet (with the corresponding mol% PS in parentheses), as a function of fX concentration. *Lines* are the single-site ligand binding equation fitted to the data. *B*, K_d values derived from binding isotherms as depicted in panel *A*. *C*, Free energies calculated from K_d values in panel *B*. *D*, R_{max} (maximal RU values) at saturating fX concentrations. Data represent mean ± S.E.M. (*n* = 3). The lower *x axes* in panels *B-D* represent the calculated number of PS molecules per leaflet, while the upper *x axes* are the mol% PS. The right *y axis* in panel *D* represents the number of fX molecules bound per leaflet, calculated as described in the text.
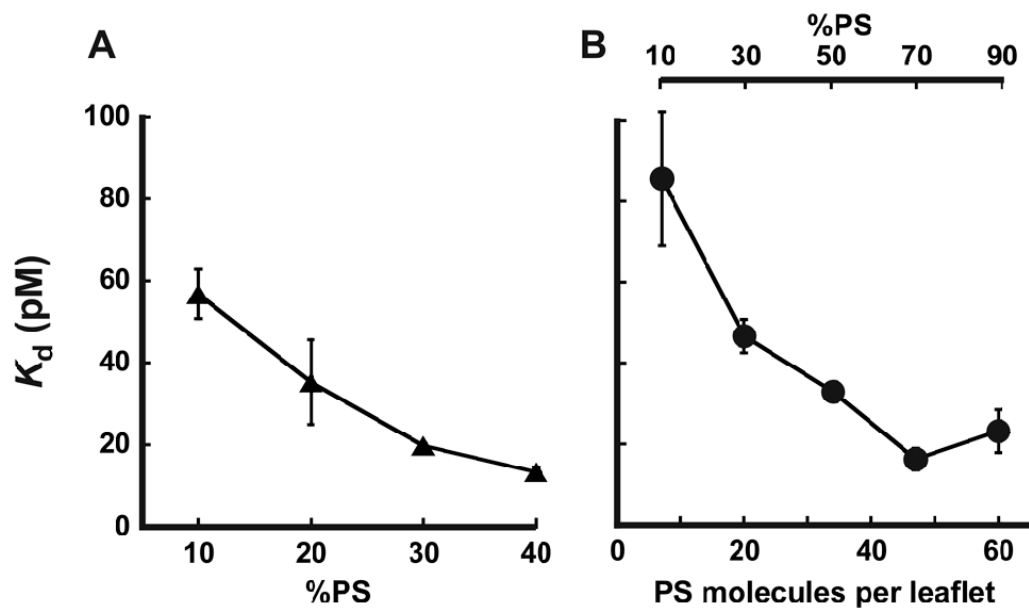
Figure 3.3   Locally high PS content supports high affinity binding of fVIIa to TF. K_d values were measured for the association of fVIIa with TF incorporated into liposomes (*A*) and Nanodiscs (*B*) as a function of PS content. The lower *x axis* in panel *B* represents the calculated number of PS molecules per leaflet, with mol% PS indicated on the upper *x axis*.
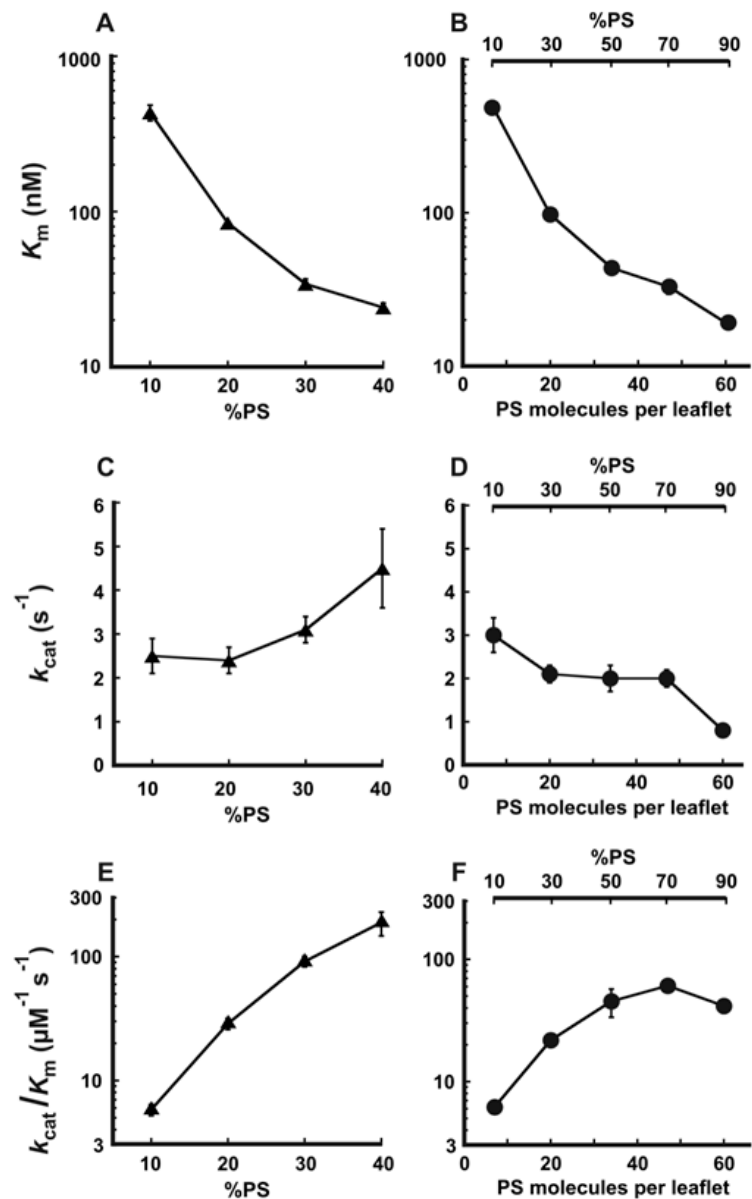
Figure 3.4   Locally high PS content promotes fX activation by TF·VIIa.
The following kinetic constants were measured for fX activation by TF·VIIa: K_m using TF-liposomes (*A*) or TF-Nanodiscs (*B*); k_{cat} using TF-liposomes (*C*) or TF-Nanodiscs (*D*); and k_{cat}/K_m using TF-liposomes (*E*) or TF-Nanodiscs (*F*). Data represent mean ± S.E.M. (*n* = 4). The lower *x axes* in panels *B, D* and *F* represent the calculated number of PS molecules per leaflet, with mol% PS indicated on the upper *x axes*. Under our experimental conditions, rates of fX activation were essentially undetectable using TF-liposomes or TF-Nanodiscs containing 100% PC, precluding their inclusion in this figure.

63

3.5 REFERENCES

1. Morrissey JH, Mutch NJ. Tissue factor structure and function. In: Colman RW, Marder VJ, Clowes AW, George JN, Goldhaber SZ (editors). *Hemostasis and Thrombosis: Basic Principles and Clinical Practice.* Philadelphia: Lippincott Williams & Wilkins, 2006; 91-106.

2. Bach RR. Initiation of coagulation by tissue factor. *CRC Crit Rev Biochem* 1988; **23:** 339-368.

3. Morrissey JH, Neuenschwander PF, Huang Q, McCallum CD, Su B, Johnson AE. Factor VIIa tissue factor: Functional importance of protein-membrane interactions. *Thromb Haemost* 1997; **78:** 112-116.

4. Lagerholm BC, Weinreb GE, Jacobson K, Thompson NL. Detecting microdomains in intact cell membranes. *Annu Rev Phys Chem* 2005; **56:** 309-336.

5. Mouritsen OG, Zuckermann MJ. What's so special about cholesterol? *Lipids* 2004; **39:** 1101-1113.

6. Haverstick DM, Glaser M. Visualization of Ca2+-induced phospholipid domains. *Proc Natl Acad Sci U S A* 1987; **84:** 4475-4479.

7. Yang L, Glaser M. Formation of membrane domains during the activation of protein kinase C. *Biochemistry* 1996; **35:** 13966-13974.

8. Del Conde I, Shrimpton CN, Thiagarajan P, Lopez JA. Tissue-factor-bearing microvesicles arise from lipid rafts and fuse with activated platelets to initiate coagulation. *Blood* 2005; **106:** 1604-1611.

9. Mandal SK, Iakhiaev A, Pendurthi UR, Rao LV. Acute cholesterol depletion impairs functional expression of tissue factor in fibroblasts: modulation of tissue factor activity by membrane cholesterol. *Blood* 2005; **105:** 153-160.

10. Sevinsky JR, Rao LVM, Ruf W. Ligand-induced protease receptor translocation into caveolae: A mechanism for regulating cell surface proteolysis of the tissue factor-dependent coagulation pathway. *J Cell Biol* 1996; **133:** 293-304.

11. Mulder AB, Smit JW, Bom VJ, Blom NR, Halie MR, van der Meer J. Association of endothelial tissue factor and thrombomodulin with caveolae. *Blood* 1996; **88:** 3667-3670.

12. Mulder KM, Humphrey LE, Gene Choi H, Childress-Fields KE, Brattain MG. Evidence for c-myc in the signaling pathway for TGF-b in well-differentiated human colon carcinoma cells. *J Cell Physiol* 1990; **145:** 501-507.

13. Krishnaswamy S, Field KA, Edgington TS, Morrissey JH, Mann KG. Role of the membrane surface in the activation of human coagulation factor X. *J Biol Chem* 1992; **267:** 26110-26120.

14. Forman SD, Nemerson Y. Membrane-dependent coagulation reaction is independent of the concentration of phospholipid-bound substrate: Fluid-phase factor X regulates the extrinsic system. *Proc Natl Acad Sci USA* 1986; **83:** 4675-4679.

15. Bom VJ, Bertina RM. The contributions of Ca^{2+}, phospholipids and tissue-factor apoprotein to the activation of human blood-coagulation Factor X by activated Factor VII. *Biochem J* 1990; **265:** 327-336.

16. Bayburt TH, Grinkova YV, Sligar SG. Self-assembly of discoidal phospholipid bilayer nanoparticles with membrane scaffold proteins. *Nano Lett* 2002; **2:** 853-856.

17. Shaw AW, McLean MA, Sligar SG. Phospholipid phase transitions in homogeneous nanometer scale bilayer discs. *FEBS Lett* 2004; **556:** 260-264.

18. Denisov IG, McLean MA, Shaw AW, Grinkova YV, Sligar SG. Thermotropic phase transition in soluble nanoscale lipid bilayers. *J Phys Chem B Condens Matter Mater Surf Interfaces Biophys* 2005; **109:** 15580-15588.

19. Leitz AJ, Bayburt TH, Barnakov AN, Springer BA, Sligar SG. Functional reconstitution of Beta2-adrenergic receptors utilizing self-assembling Nanodisc technology. *BioTechniques* 2006; **40:** 601-2, 604, 606, passim.

20. Bayburt TH, Sligar SG. Self-assembly of single integral membrane proteins into soluble nanoscale phospholipid bilayers. *Protein Sci* 2003; **12:** 2476-2481.

21. Smith SA, Morrissey JH. Rapid and efficient incorporation of tissue factor into liposomes. *J Thromb Haemost* 2004; **2:** 1155-1162.

22. Waters EK, Morrissey JH. Restoring full biological activity to the isolated ectodomain of an integral membrane protein. *Biochemistry* 2006; **45:** 3769-3774.

23. Wilschut J, Duzgunes N, Hoekstra D, Papahadjopoulos D. Modulation of membrane fusion by membrane fluidity: temperature dependence of divalent cation induced fusion of phosphatidylserine vesicles. *Biochemistry* 1985; **24:** 8-14.

24. Banner DW, D'Arcy A, Chène C, Winkler FK, Guha A, Konigsberg WH, Nemerson Y, Kirchhofer D. The crystal structure of the complex of blood coagulation factor VIIa with soluble tissue factor. *Nature* 1996; **380:** 41-46.

25. Small DM. Phase equilibria and structure of dry and hydrated egg lecithin. *J Lipid Res* 1967; **8:** 551-557.

26. Denisov IG, Grinkova YV, Lazarides AA, Sligar SG. Directed self-assembly of monodisperse phospholipid bilayer Nanodiscs with controlled size. *J Am Chem Soc* 2004; **126:** 3477-3487.

27. Neuenschwander PF, Morrissey JH. Roles of the membrane-interactive regions of factor VIIa and tissue factor. The factor VIIa Gla domain is dispensable for binding to tissue factor but important for activation of factor X. *J Biol Chem* 1994; **269:** 8007-8013.

28. Neuenschwander PF, Bianco-Fisher E, Rezaie AR, Morrissey JH. Phosphatidylethanolamine augments factor VIIa-tissue factor activity: Enhancement of sensitivity to phosphatidylserine. *Biochemistry* 1995; **34:** 13988-13993.

29. Nelsestuen GL, Broderius M. Interaction of prothrombin and blood-clotting factor X with membranes of varying composition. *Biochemistry* 1977; **16:** 4172-4177.

30. Hathcock JJ, Rusinova E, Gentry RD, Andree H, Nemerson Y. Phospholipid regulates the activation of factor X by tissue factor/factor VIIa (TF/VIIa) via substrate and product interactions. *Biochemistry* 2005; **44:** 8187-8197.

31. Terrettaz S, Stora T, Duschl C, Vogel H. Protein binding to supported lipid membranes: Investigation of the cholera toxin-ganglioside interaction by simultaneous impedance spectroscopy and surface plasmon resonance. *Langmuir* 1993; **9:** 1361-1369.

32. Heyse S, Vogel H, Sanger M, Sigrist H. Covalent attachment of functionalized lipid bilayers to planar waveguides for measuring protein binding to biomimetic membranes. *Protein Sci* 1995; **4:** 2532-2544.

33. Andree HAM, Contino PB, Repke D, Gentry R, Nemerson Y. Transport rate limited catalysis on macroscopic surfaces: The activation of factor X in a continuous flow enzyme reactor. *Biochemistry* 1994; **33:** 4368-4374.

34. Hathcock JJ, Rusinova E, Andree H, Nemerson Y. Phospholipid surfaces regulate the delivery of substrate to tissue factor:VIIa and the removal of product. *Blood Cells Mol Dis* 2006; **36:** 194-198.

35. Krishnaswamy S. Exosite-driven substrate specificity and function in coagulation. *J Thromb Haemost* 2005; **3:** 54-67.

CHAPTER 4

INFLUENCE OF THE LOCAL PHOSPHOLIPID NANOENVIRONMENT ON PROTHROMBINASE FUNCTION

4.1 BACKGROUND

Prothrombin is converted to thrombin by the serine protease, factor Xa (fXa), in complex with its protein cofactor, factor Va (fVa) [1,2]. This complex of fVa and fXa – often called prothrombinase – assembles in a Ca^{2+}-dependent manner on suitable membrane surfaces [3,4]. In addition to providing a platform for prothrombinase assembly, biological membranes also modulate the catalytic activity of prothrombinase and other serine protease-cofactor complexes in blood clotting [5]. Studies using liposomes and other model membranes have shown that anionic phospholipids are required for optimal prothrombinase activity, with phosphatidylserine (PS) being the most active [5,6]. Unfortunately, the mechanisms by which PS enhances the enzymatic activity of prothrombinase – or indeed any other protease-cofactor complex in blood clotting – are not fully understood.

We hypothesize that prothrombinase and other blood clotting protease-cofactor complexes partition into membrane microdomains of locally very high PS content. Studies of giant unilamellar vesicles composed of mixtures of anionic and neutral phospholipids have shown that plasma concentrations of Ca^{2+} can induce anionic phospholipids to move over relatively long distances to cluster into anionic phospholipid-rich membrane domains. Clustering of anionic phospholipids was even more dramatic when vesicles were treated with

68

combinations of Ca^{2+} and proteins known to bind to anionic phospholipids, such that the membrane-binding proteins co-clustered with anionic phospholipids [7,8]. It therefore seems likely that blood clotting reactions occur preferentially on membrane surfaces containing locally high PS content, which may result from both calcium ions and the PS-binding properties of the proteins themselves. Unfortunately, when using even simple model membranes, it is very difficult to know the phospholipid composition immediately surrounding the membrane-bound prothrombinase complex and its membrane-bound substrate, prothrombin. In the presence of plasma concentrations of Ca^{2+}, liposomes composed of 20% PS and 80% phosphatidylcholine (PC) are likely to segregate into a patchwork of microenvironments in which the local PS content at any given point may be considerably higher or lower than the average of 20%. Thus, local variations in the membrane nanoenvironment immediately surrounding prothrombinase may dramatically alter its catalytic efficiency. When using liposomes or other model membranes, this parameter is typically not under experimental control.

In the present study, we used supported nanometer-scale phospholipid bilayers (Nanodiscs) of defined size and phospholipid composition as the experimental membrane surface upon which to assemble and study the components of the prothrombinase complex. Nanodiscs are water-soluble bilayers encircled and stabilized by an amphipathic helical protein termed membrane scaffold protein (MSP). The nanobilayers within Nanodiscs are monodisperse and exhibit lipid fluidity comparable to liposomes [9,10]. Nanodiscs self-assemble from mixtures of phospholipid and MSP, yielding stabilized

nanoscale bilayers whose lipid composition is under strict experimental control. Newer-generation Nanodiscs have been developed using MSPs that have been systematically elongated or truncated to yield stabilized, monodisperse phospholipid bilayers ranging from about 8 to 15 nm in diameter [11]. By assembling the constituent proteins of the prothrombinase complex on these nanobilayers, we can circumvent the long-range recruitment of anionic phospholipids that occurs in larger phospholipid systems such as liposomes. This affords us complete control over the composition of the membrane nanoenvironment immediately surrounding the prothrombinase complex. Our results now demonstrate how locally high PS concentrations regulate prothrombinase assembly and function.

4.2   EXPERIMENTAL PROCEDURES

4.2.1   Materials

PC (1-palmitoyl-2-oleoyl-*sn*-glycero-3-phosphocholine), PS (1-palmitoyl-2-oleoyl-*sn*-glycero-3-phosphoserine) and the lipid extruder were from Avanti Polar Lipids (Alabaster, AL). Benzamidine was from Fisher Scientific (Pittsburg, PA). Human prothrombin and fXa were from Enzyme Research Laboratories (South Bend, IN). DAPA (dansylarginine N-(3-ethyl-1,5-pentanediyl)amide) and fVa were from Haematological Technologies, Inc. (Essex Junction, VT). Nanodisc Membrane Scaffold Proteins, MSP1D1 and MSP1E3D1 were expressed in *E. coli* and purified as previously described [12].

4.2.2 Surface Plasmon Resonance Analyses

Binding of prothrombin, fXa and fVa to Nanodiscs of varying mol% PS was quantified by surface plasmon resonance using a Biacore 3000 instrument and NTA Sensor Chips (Piscataway, NJ) as described [13], with the following modifications: After the NTA chips were charged with Ni^{2+}, Nanodiscs containing a 6xHis tag in the MSP were loaded onto each channel in calcium-free running buffer until a signal of 600 to 800 RU was achieved. A steady baseline was then established in running buffer (10 mM HEPES-NaOH pH 7.4, 150 mM NaCl, 2.5 mM $CaCl_2$), after which increasing concentrations of the desired protein were injected. Upon reaching steady-state binding, the maximal RU response above baseline was recorded. The single-site ligand binding equation was fitted to these steady-state RU values to calculate the K_d of protein binding to the nanoscale bilayers. Membrane binding of fXa and prothrombin was quantified using Nanodiscs with 7.7 nm-diameter bilayers as described for factor X [13], except that 5 mM benzamidine was included in the buffers when fXa was used. Membrane binding of fVa was quantified using Nanodiscs with 10.8 nm-diameter bilayers.

The numbers of protein molecules (prothrombin, fXa, or fVa) bound at saturation per Nanodisc leaflet were calculated by assuming that protein and phospholipid bilayers have equivalent effect on refractive index, as has been previously demonstrated [13-15]. The molar ratio of bound protein molecules to Nanodiscs at saturation equals $(RU_{protein}/RU_{Nanodisc})*(MW_{Nanodiscs}/MW_{protein})$, with $RU_{Nanodiscs}$ corresponding to the amount of Nanodiscs loaded onto the sensorchip,

and $RU_{protein}$ corresponding to the amount bound analyte at saturation (the latter calculated from the fitted single-site ligand binding equation). $MW_{protein}$ corresponds to the molecular weights of the proteins of interest: 173 kDa for fVa, 46 kDa for fXa, and 72 kDa for prothrombin. $MW_{Nanodiscs}$ is the sum of the constituent masses. The molecular weight of MSP1D1 is 24.7 kD and of MSP1E3D1 is 32.6 kDa, with two copies of each MSP per Nanodisc. The molecular weights of PC and PS are 760 and 784 Da, and there are 134 or 240 phospholipid molecules per 7.7 or 10.8 nm-diameter bilayer, respectively.

4.2.3 Rates of Prothrombin Activation

Initial rates of prothrombin activation by the prothrombinase complex, assembled either on liposomes or Nanodiscs (10.8 nm-diameter bilayers) of varying mol %PS, were quantified using a continuous DAPA-based prothrombin activation assay [16,17]. Briefly, prothrombin activation reactions were conducted in HEPES-buffered saline (20 mM HEPES-NaOH pH 7.4, 150 mM NaCl, 2.5 mM $CaCl_2$, 0.1% polyethylene glycol 8000) containing 4.5 nM fVa, 10 µM DAPA, varying prothrombin concentrations and either liposomes (5 µM phospholipid) or 10.8 nm-diameter Nanodiscs (2.5 µM phospholipid). Thrombin generation was initiated by adding 60 pM fXa, and DAPA fluorescence was monitored over time (excitation at 280 nm, emission at 545 nm, and cutoff at 515 nm) using a Spectramax Gemini XS microplate fluorometer (Molecular Devices; Sunnyvale, CA). K_m and k_{cat} values were calculated by fitting the Michaelis-Menten equation to the rate data using nonlinear regression.

Prothrombin activation by prothrombinase occurs via cleavage of two peptide bonds with two possible intermediates: meizothrombin, or prethrombin 2 [17]. To determine the intermediates of prothrombin cleavage, reaction mixtures containing 4.5 nM fVa, 60 pM fXa, 1 µM prothrombin and 10 µM DAPA were activated on phospholipids (either 5 µM liposomes or 2.5 µM Nanodiscs with 10.8 nm-diameter bilayers) in HEPES-buffered saline. Samples were quenched at fixed time points in 50 mM EDTA, heated to 90°C for 5 min, and resolved on SDS-PAGE. Bands were detected by staining with Coomassie.

4.3   RESULTS

In this study we investigated how the membrane composition *immediately* surrounding prothrombinase modulates its assembly and enzymatic activity. To accomplish this we assembled the components of the prothrombinase complex on nanoscale phospholipid bilayers (Nanodiscs) of controlled phospholipid composition. Unlike liposomes and most other model membrane systems, the phospholipid bilayers in Nanodiscs cannot undergo long-range, Ca^{2+}-induced reorganization of PS molecules into regions of locally high PS content, which allows us to define the membrane composition immediately under and surrounding prothrombinase. In our recent study of assembling the tissue factor-factor VIIa complex on nanoscale bilayers, we found that 7.7 nm-diameter bilayers were large enough to accommodate fully functional tissue factor-factor VIIa complexes, allowing us to measure high rates of factor X activation [13]. The prothrombinase complex is larger than the tissue factor-factor VIIa complex, however, chiefly because fVa is about four times the size of tissue factor. We

therefore found that assembling the complete prothrombinase complex required the use of Nanodiscs containing 10.8 nm-diameter bilayers. On the other hand, we could readily quantify binding of fXa or prothrombin to nanobilayers to Nanodiscs containing 7.7 nm-diameter bilayers.

4.3.1 Size Considerations

In order to employ Nanodiscs to study the assembly and function of the prothrombinase complex, it was necessary to determine that the supported nanoscale bilayers have sufficient surface area to accommodate both fVa and fXa, and also to bind at least one substrate molecule (prothrombin). It should be pointed out that the membrane binding domains of these proteins have relatively small cross-sectional areas, while the larger, globular portions of fVa, fXa and prothrombin are free to project beyond the boundaries of the supported bilayers. Using individual crystal structures of the Gla domain of bovine fXa [18] and both C domains of bovine fVai [19], we created a schematic of the membrane contact domains of the constituent partner proteins of prothrombinase on a 7.7 and 10.8 nm-diameter Nanodisc. As displayed in Fig. 4.1*A*, the smaller 7.7 nm-diameter bilayer seems unlikely to support the entire complex. However, the 10.8 nm-diameter bilayer visually demonstrates that there should be sufficient room to accommodate prothrombinase and to bind multiple substrate molecules as well (Fig. 4.1*B*).

4.3.2 Binding of Prothrombin to PS-Containing Bilayers

An essential function of PS is to promote binding of substrate (prothrombin) to the membrane surface in the vicinity of the prothrombinase complex. Accordingly, we used surface plasmon resonance to quantify the binding of prothrombin to immobilized nanoscale bilayers as a function of PS content. Previously, we used immobilized Nanodiscs containing 7.7 nm-diameter bilayers to quantify PS-dependent fX binding [13], so we also chose to use Nanodiscs of this size for studying the effects of PS content on membrane binding of prothrombin. Fig. 4.2*A* shows representative plots of steady-state RU values for binding of prothrombin to Nanodiscs of varying PS content. No appreciable prothrombin binding to Nanodiscs containing 100% PC was detected, but as the PS content increased, prothrombin bound to the nanoscale bilayers in a saturable, concentration-dependent manner. The single-site ligand binding equation fit well to the data in Fig. 4.2*A*, yielding K_d values that decreased monotonically as the PS content increased (Fig. 4.2*B*). This corresponded to a monotonic increase in binding energy with increasing PS content (Fig. 4.2*C*). The K_d values we obtained from Nanodiscs containing 60 to 100% PS are within the range of literature values for prothrombin binding to liposomes composed of 20 to 30% PS [5].

We used the binding data from Fig. 4.2*A* to calculate the number of prothrombin molecules bound per leaflet, plotted in Fig. 4.2*D* as a function of PS content. At saturation, a maximum of about 8 prothrombin molecules can bind per 7.7 nm-diameter leaflet composed of 100% PS, which corresponds to about

one prothrombin binding site per 8.3 PS molecules. This is nearly identical to the maximal number of fX molecules bound per 7.7 nm-diameter bilayer composed of 100% PS [13].

4.3.3 Binding of fXa to PS-Containing Bilayers

We next investigated the effect of local PS content on the membrane binding affinity of the components of the prothrombinase complex, starting with fXa. Using the same surface plasmon resonance approach that we used to quantifying prothrombin binding, we found that no appreciable fXa bound to nanoscale bilayers containing 100% PC. As the PS content increased, however, fXa bound to the nanobilayers in a saturable, concentration-dependent manner (Fig. 4.3A). The single-site ligand binding equation fit well to the data (Fig. 4.3A), yielding K_d values that decreased as the PS content increased from 20 to 60%, but which were relatively constant from 60 to 100% PS (Fig. 4.3B). The relationship between fXa binding and PS content is seen more clearly when binding energies are plotted as a function of PS content (Fig. 4.3C). For comparison purposes we have also plotted, in Figs. 4.3B and 4.3C, data for binding of zymogen fX to 7.7 nm-diameter nanobilayers collected under identical conditions [13]. The most striking difference between fX and fXa binding is that fXa exhibited higher binding affinity for nanobilayers from 20 to 60% PS, while the binding affinities of fX and fXa were essentially the same at high PS content (80 and 100% PS).

The calculated maximal number of fXa molecules bound per nanobilayer were plotted in Fig. 4.3D as a function of PS content. Interestingly, at saturation

the nanobilayers bound more than twice as many fXa molecules per leaflet compared with fX, at all PS contents tested (Fig. 4.3D). Thus, a maximum of approximately 20 fXa molecules were found to bind to a 7.7 nm-diameter leaflet composed of 100% PS. This compares to only about 8 fX molecules per leaflet on the same type of surface, a difference in binding capacity of about 2.5-fold. The calculated number of PS molecules per protein at saturation is 3.4 PS molecules per fXa and 8.4 PS molecules per fX.

4.3.4 Binding of fVa to PS-Containing Bilayers

The other half of the prothrombinase complex is fVa, so we examined the PS-dependence of fVa binding to nanobilayers. In initial surface plasmon resonance experiments, we observed only weak binding of fVa to Nanodiscs containing 7.7 nm-diameter bilayers, but much stronger binding to Nanodiscs containing 10.8 nm-diameter bilayers (not shown). We therefore quantified fVa binding to the larger Nanodiscs as a function of PS content. We found no appreciable fVa binding to bilayers containing 100% PC, and very limited fVa binding at 10% PS (Fig. 4.4A). From 20 to 90% PS, however, fVa bound in a saturable, concentration-dependent manner, and the single-site ligand binding equation fit well to the data. The K_d values for fVa binding to PS-containing nanobilayers varied by only a small amount from 10 to 90% PS (Fig. 4.4B), reflected in relatively small changes in binding energy (Fig. 4.4C). At saturation, we found that a maximum of about 2 to 2.5 fVa molecules were bound per 10.8 nm-diameter leaflet composed of 20-90% PS (Fig. 4.4D). This corresponds to about one fVa binding site per 10 PS molecules when the nanobilayer contained

20% PS. Bilayers with 10% PS bound very little fVa, suggesting that such bilayers lacked the minimum number of PS molecules to productively bind fVa.

4.3.5 Prothrombin Activation on Nanoscale Bilayers

The influence of local PS content on prothrombinase activity was investigated by assembling the prothrombinase complex on 10.8 nm-diameter bilayers of varying PS composition. A stoichiometric excess of Nanodiscs to fVa molecules was used to minimize the occurrence of more than one fVa molecule bound per Nanodisc leaflet. For comparison, the prothrombinase complex was also assembled on liposomes of varying PS content. On liposomes, the K_m for prothrombin activation by prothrombinase dropped about two-fold between 8 and 10% PS, and then decreased much more modestly as the PS content was further increased to 40% PS (Fig. 4.5A). On Nanodiscs, the K_m was equally high at 10 and 20% PS, but decreased almost linearly as the PS content increased to 70% (Fig. 4.5B). The lowest K_m on Nanodiscs was achieved at 70% PS, and was essentially equivalent to the K_m obtained using liposomes containing 20 to 40% PS.

The k_{cat} values for prothrombin activation by prothrombinase on liposomes varied relatively little when liposomes contained 8 to 40% PS, but showed a maximum at 20% PS (Fig. 4.5C). On Nanodiscs, k_{cat} was somewhat lower than on liposomes, and also varied somewhat more than on liposomes (Fig. 4.5D). Thus, on Nanodiscs k_{cat} was maximal at 20% PS and then decreased almost linearly as the PS content increased from 30 to 70%.

On liposomes, k_{cat}/K_m increased from 8 to 30%, and then decreased slightly at 40% PS (Fig. 4.5*D*). In contrast, on Nanodiscs k_{cat}/K_m increased almost linearly as the PS content increased from 10 to 70% PS (Fig. 4.5*E*).

4.4   DISCUSSION

4.4.1 The Local PS Environment Influences the Binding of Prothrombin, fXa, and fVa to Membranes

We have found that prothrombin, fXa and fVa are dependent on high local concentrations of PS for high affinity membrane binding. By calculating the stoichiometric ratio of the number of protein molecules bound per leaflet of the Nanodisc from surface plasmon resonance data, we observed that as the PS content was raised, more proteins bind the membrane in a saturable, concentration-dependent manner. We have found that the maximal amount of prothrombin bound at steady-state increased linearly as a function of PS content in 7.7 nm diameter bilayer Nanodiscs. At saturation, 8 prothrombin molecules bound a 67 phospholipid leaflet composed of 100% PS (*i.e.,* 16 prothrombin molecules per 7.7 nm diameter Nanodisc containing a total of 134 phospholipids). This is consistent with our recent manuscript in which we demonstrated how 8 fX molecules bound a 67 phospholipid leaflet composed of 100% PS [13]. It is of note that the two serine protease zymogens we have so far evaluated, fX and prothrombin, have footprints that cover the same amount of phospholipid headgroups.

Our surface plasmon resonance studies with fXa showed that, at saturation, a total of ~20 fXa molecules were found on a 7.7nm diameter bilayer

Nanodisc leaflet; approximately twice the amount found for its zymogen form, fX. This suggests that, in the presence of Ca^{2+} and on a membrane bilayer composed of 100%PS, fXa can occupy twice the phospholipid surface area of fX. The two cleavage events that activate fX into fXa release an activation peptide fragment. The release of this peptide renders fXa 20% smaller than fX by molecular weight. Moreover, since the cleavage events are distal to the GLA domain, no considerable conformational changes in the GLA domain are predicted to occur. As discussed above, we have estimated that a 7.7 nm diameter membrane composed of only 67 phospholipids can bind, at a theoretical maximum, 10 to maybe 13 GLA domains. This prediction does not however take into account the entire protein, but only its membrane binding portion. Our results, therefore, exceed our maximal estimate for the GLA domain alone by a factor of ~2. Taken together, it is unlikely that the neither cleavage events alone, nor does a conformation change in the GLA domain account for the increase in the density of fXa compared to fX on the membrane surface. The two-fold increase in the lipid density of fXa, however, is highly suggestive that membrane-bound fXa is very efficiently packed and/or is dimerizing on the phospholipid surface. Interestingly, a recent study by Hathcock, *et al.* [20], also supports this hypothesis. Briefly, the authors also showed that the maximum lipid binding capacity of fXa exceeded that of fX by a factor of two. It was proposed that if fXa is indeed a monomer, it packs onto a membrane bilayer with extreme efficiency; nearly comparable to highly organized, hexagonally packed cylinders [20]. The authors suggest that although it is not impossible to pack proteins in

this manner, an alternative hypothesis is that the fXa molecule dimerizes on the membrane surface. In their model, the first fXa molecule binds phospholipids, while the second binds the first fXa molecule; effectively reducing the apparent number of phospholipids that fXa binds to in half. The fXa dimer model has also been previously proposed [21,22] and it has been speculated that dimerization of fXa serves to increase its phospholipid density. In turn, the high density of fXa may serve to out-compete fX and other substrates from the membrane surface. Perhaps coincidentally, our binding data also shows that compared to fX, fXa has a higher affinity for membranes containing low amounts of PS and equivalent affinity when the membrane has high PS content; hinting at the existence of a form of competitive mechanism between the fX and fXa on the membrane surface.

The fVa molecule binds membranes via electrostatic and hydrophobic interactions [23-25] through an incompletely understood mechanism. Although fVa will bind membranes composed of pure PC, the reported K_d for this interaction is very weak (3 µM), and at least 2 orders of magnitude beyond the reported plasma concentration of fVa [26,27]. In order for fVa to bind membranes with high affinity and physiological relevance, PS molecules are required. Reportedly, as little as 10 PS molecules are needed for one fVa molecule to bind membranes [28]. Indeed, with our experimental conditions, we were able to detect binding with as little as ~12 PS molecules (the lowest PS content we evaluated) and we estimate that one fVa molecule will bind anywhere between 12 to 24 PS molecules (Fig. 4.4*D*). As such, to achieve binding at physiological

81

levels, a minimum amount of PS molecules are simply required. Once binding

has occurred, there is however, very little change in K_d as PS content is raised.

We speculate that the qualitative changes in K_d values are largely due the

inefficiency of fVa access to PS binding sites on a constrained nanobilayer. To

elaborate, as the PS content of the Nanodiscs is increased, more fVa binding

sites become available. However, because the size of the bilayer remains the

same, fVa molecules must then compete for space in order to saturate the

remaining binding sites. Indeed, as observed in Fig. 4.4D, a 10.8 nm diameter

bilayer composed of 90% PS becomes saturated when only about 3 fVa

molecules bind. This competition of PS binding sites within a limited surface area

may account for the slight increase in the K_d for the interaction of fVa to

membranes.

On a resting cell or platelet surface, PS and other aminophospholipids are

sequestered within the inner cell membrane and away from the circulation, while

choline phospholipids such as PC are sequestered on the outer leaflet [3,29].

Upon cell damage or induction of other stressors, PS molecules are scrambled

onto the outer leaflet. This manuscript and others have established that the

binding of many plasma-derived blood coagulation proteins are PS dependent.

Our results show no detectable binding of fVa to membranes in the absence of

PS molecules. However, after a minimal number of PS molecules are reached,

fVa begins to bind PS-containing membranes at high affinity, and below the total

physiological concentration of its unactivated form, fV. A relatively small amount

of PS (12-24 molecules) on the membrane surface is sufficient to induce high

affinity binding of fVa. This supports the oft-proposed idea that once bound to a membrane, fVa is responsible for priming the assembly of the prothrombinase complex [5]. We also show that the high affinity binding of fXa and prothrombin to membranes occur at a very high PS content. Likewise, the optimal K_d values of these vitamin K-dependent proteins are near or below the reported plasma concentrations of their zymogen forms. Taken together, we propose that in the absence of stress, these zymogens remain at equilibrium between their membrane-bound and solution-state species. However, stress triggers the release of PS molecules on a membrane surface. At high enough concentrations, these PS molecules become tightly packed, which in turn creates more high affinity binding sites. As a result, the K_d for membrane binding drops below the plasma concentration, and pushes the equilibrium of these proteins towards their membrane-bound states. By increasing the affinities of these proteins for membranes, PS molecules contribute to increasing the overall density of these proteins on the membrane surface, and at the nanoscale level, this increased density may be very substantial. Others have proposed that proteins in the vicinity of the membrane surface may be orders of magnitude greater than those observed in the bulk solution [5]. This high local concentration of proteins within a constrained volume may in turn substantially and positively affect prothrombinase complex formation and function [30-32].

4.4.2 Prothrombinase Complex Function is Regulated by its Local PS Environment

Nanodiscs provide a system in which we can more easily control and resolve the phospholipid environment in the immediate vicinity of a protein. To determine, at the nanoscale, how prothrombinase is modulated by PS, we assembled the complex and its substrate on liposomes or 10.8 nm diameter bilayer Nanodiscs and compared their functions. Our experiments show that the K_m for prothrombinase function on liposomes became optimal at very low PS content (10%PS). The K_m for prothrombinase function on Nanodiscs, however, decreased steadily as more PS molecules were gradually incorporated into the bilayer. Only at a very high PS content (70%) did K_m values on Nanodiscs become equivalent with liposomes containing 10-40%PS. We reason that because Nanodiscs prevent long-range recruitment of PS, the immediate vicinity of the prothrombinase complex can be effectively titrated with PS molecules as PS content is raised. This degree of control, in turn, gives us a more accurate description of the actual PS composition in the immediate vicinity of the prothrombinase complex. On the other hand, liposomes can contain ~200 times more phospholipid molecules than Nanodiscs. Evident from the maximal K_m values at very low %PS (Fig. 5A), phospholipid domains with optimal PS content for activating prothrombin by prothrombinase can effectively form on ~100 nm diameter liposomes with as little as 10% PS. Taken together, these results show that there an extremely high content of PS is required for maximal prothrombinase function. Even with their constrained size, Nanodiscs can effectively support the function of the prothrombinase complex if a very high

amount of PS in incorporated into the bilayer. This requirement for high PS is masked in liposomes because its phospholipid surface has the propensity to form domains that extremely rich in PS molecules.

We have described how the prothrombinase complex can effectively assemble and activate its natural protein substrate, prothrombin, on a nanometer-scale bilayer that contains only 120 phospholipids molecules per leaflet. To generate full function, no less than three proteins are needed to bind on the same PS-containing membrane surface. As such, a requisite amount of PS incorporated into the membrane is required to bind each protein molecule. We have estimated that in order for a single molecule of prothrombin, factor Xa, and factor Va to bind membranes with high affinity, approximately 9, 4, and less than 24 PS molecules are required for each protein respectively. Taken together, these results indicate that approximately 37 PS molecules are required for optimal assembly of the prothrombinase complex and its substrate. Although this estimate does not take into account interactions that may affect the net amount of PS required, it is interesting to note that maximal k_{cat} values for prothrombin by prothrombinase on 10.8 nm-diameter bilayer Nanodiscs also occurs between 24-36 PS molecules (Fig. 4.5*D*). Compared to liposomes, however, prothrombin activation was found to be less efficient on the constrained bilayer of the Nanodiscs. A drop in prothrombin turnover rates on Nanodiscs can also be seen at very high PS content. Thus, the size and density of anionic phospholipids within a membrane can contribute greatly to the efficiency of substrate turnover. Indeed, studies prior have shown that mixtures of PC and PS are more effective

in promoting thrombin generation than PC or PS membranes alone [33,34]; indicating that an optimal amount of PS molecules are required for maximal prothrombinase turnover.

Many blood coagulation serine proteases and their subsequent protease:cofactor complexes have evolved binding sites to regulate their functions. At the fundamental level, these "exosites" may be anywhere in the vicinity of the complex, yet outside its active site. Indeed, in a previous manuscript, we described how the extrinsic tenase complex, another membrane-bound blood coagulation complex, uses anionic phospholipids as exosites to enhance the binding affinity of its protein substrates [13]. In a similar manner, we propose that the PS molecules located within nanometers of the prothrombinase complex serve as an exosite to regulate its assembly and function.
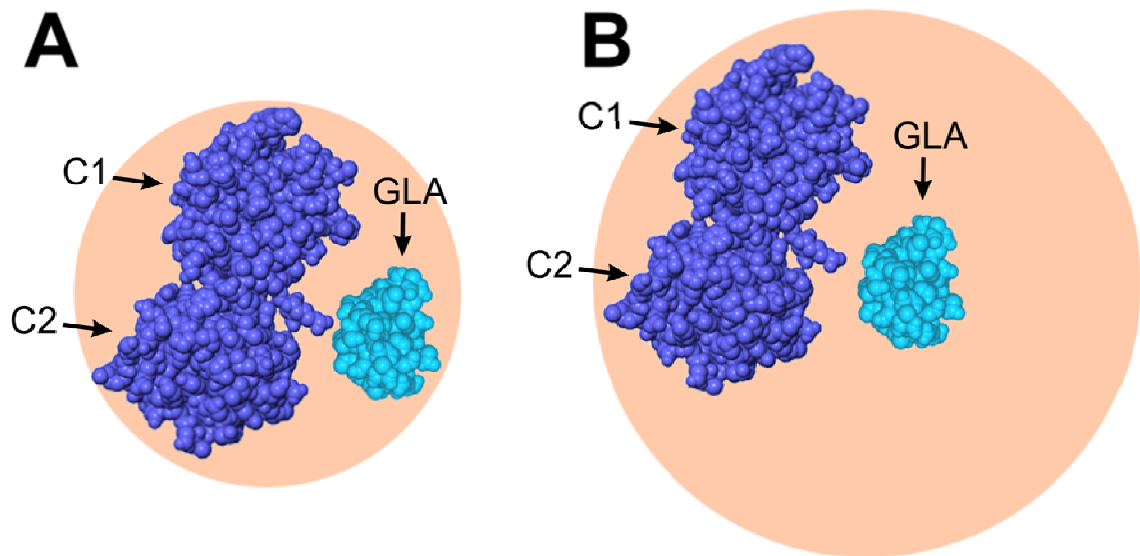
Figure 4.1   Schematic of the membrane contact domains of fVa and fXa on nanoscale bilayers. The C1 and C2 domains of bovine fVa in *blue* (PDB file 1SDD [19]) and the Gla domain of fXa is in *cyan* (PDB file 1IOD [18]) are placed, to scale, on nanoscale bilayers (*tan circles*) of 7.7 nm diameter (*panel A*), or 10.8 nm diameter (*panel B*). The 10.8 nm-diameter bilayer appears highly likely to have sufficient room to assemble the prothrombinase complex (Va·Xa) and one or more substrate molecules. The smaller 7.7 nm-diameter bilayer seems unlikely to support the entire complex and substrate.
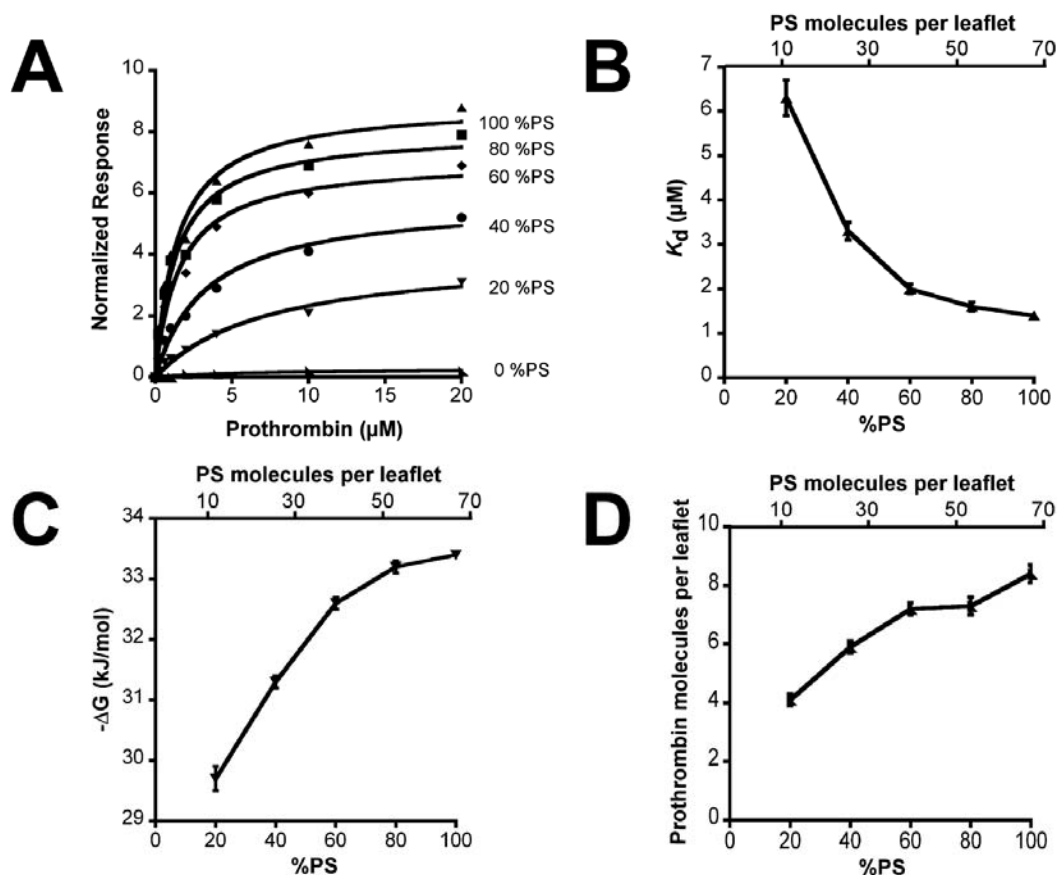
Figure 4.2   Binding of prothrombin to 7.7 nm-diameter bilayer Nanodiscs of varying PS content, measured by surface plasmon resonance. *A*, steady-state binding of prothrombin to Nanodiscs of indicated %PS as a function of prothrombin concentration. *Lines* are the single-site ligand binding equation fitted to the data. *B*, K_d values derived from binding isotherms depicted in *A*, as a function of PS content. *C*, calculated negative free energy change for prothrombin bind as a function of PS content (derived from K_d values in *B*). *D*, The number of prothrombin molecules bound per leaflet at saturating prothrombin concentrations, calculated as described in text. Data represent mean ± S.E. ($n \geq 3$). The *upper x axes* in *B - D* represent the calculated number of PS molecules per leaflet, whereas the *lower x axes* are the mol % of PS.
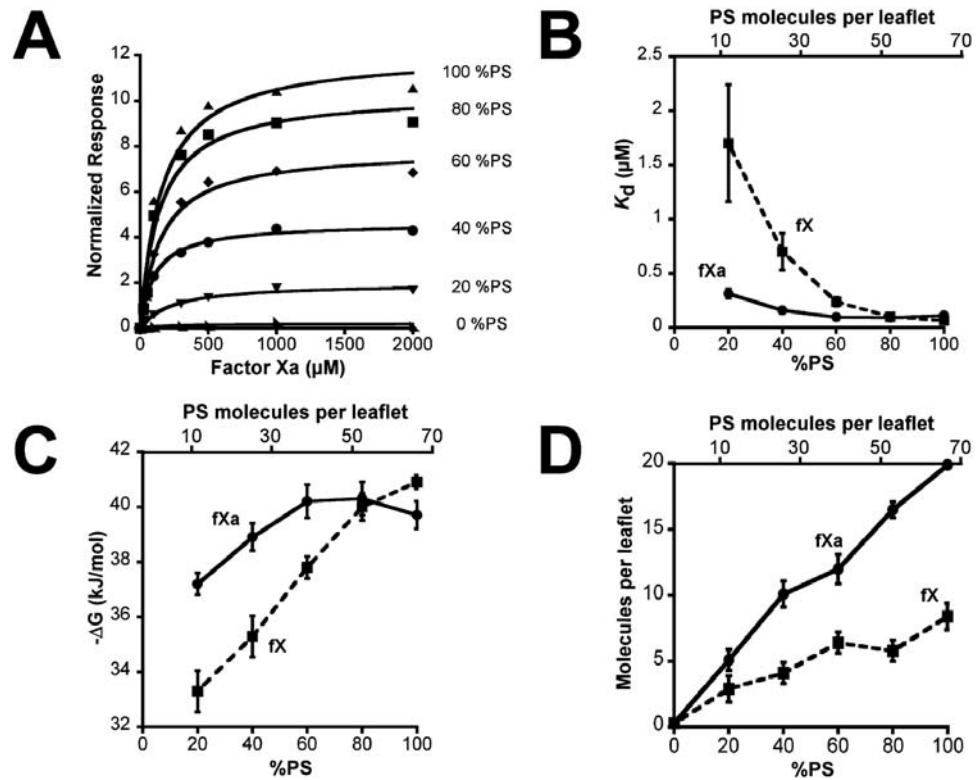
Figure 4.3   Binding of fXa and fX to 7.7 nm-diameter bilayer Nanodiscs of varying PS content, measured by surface plasmon resonance. *A*, steady-state binding of fXa to Nanodiscs of indicated %PS as a function of fXa concentration. *Lines* are the single-site ligand binding equation fitted to the data. *B*, K_d values for fXa (*circles, solid line*) derived from binding isotherms depicted in *A*, as a function of PS content. K_d values for fX (*squares, dotted line*) were replotted from Shaw et al. [13], and are overlaid here for comparison. *C*, calculated free energy change for fXa and fX binding as a function of PS content (derived from K_d values in *B*, and from Shaw *et al*. [13]. *D*, The number of fXa and fX molecules bound per Nanodisc leaflet at saturating fX or fXa concentrations, calculated as described in text or replotted from Shaw *et al*., 2007. Data represent mean ± S.E. (*n* = 3). The *upper x axes* in *B - D* represent the calculated number of PS molecules per leaflet, whereas the *lower x axes* are the mol % of PS.
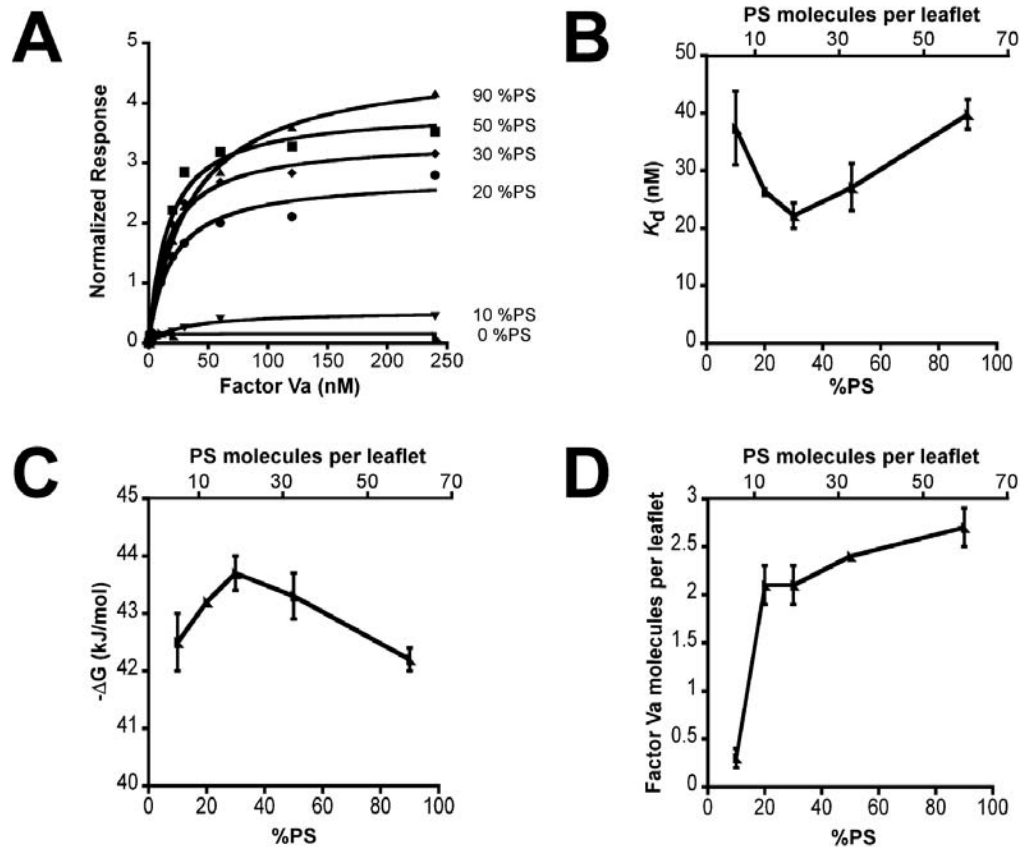
Figure 4.4   Binding of fVa to 10.8 nm-diameter bilayer Nanodiscs of varying PS content, measured by surface plasmon resonance. *A*, steady-state binding of fVa to Nanodiscs of indicated %PS as a function of fVa concentration. *Lines* are the single-site ligand binding equation fitted to the data. *B*, K_d values derived from binding isotherms depicted in *A*, as a function of PS content. *C*, calculated free energy changes for fVa binding as a function of PS content (derived from K_d values in *B*). *D*, The number of fVa molecules bound per Nanodisc leaflet at saturating fVa concentrations, calculated as described in text. Data represent mean ± S.E. (*n* = 3). The *upper x axes* in *B - D* represent the calculated number of PS molecules per leaflet, whereas the *lower x axes* are the mol % of PS.

90
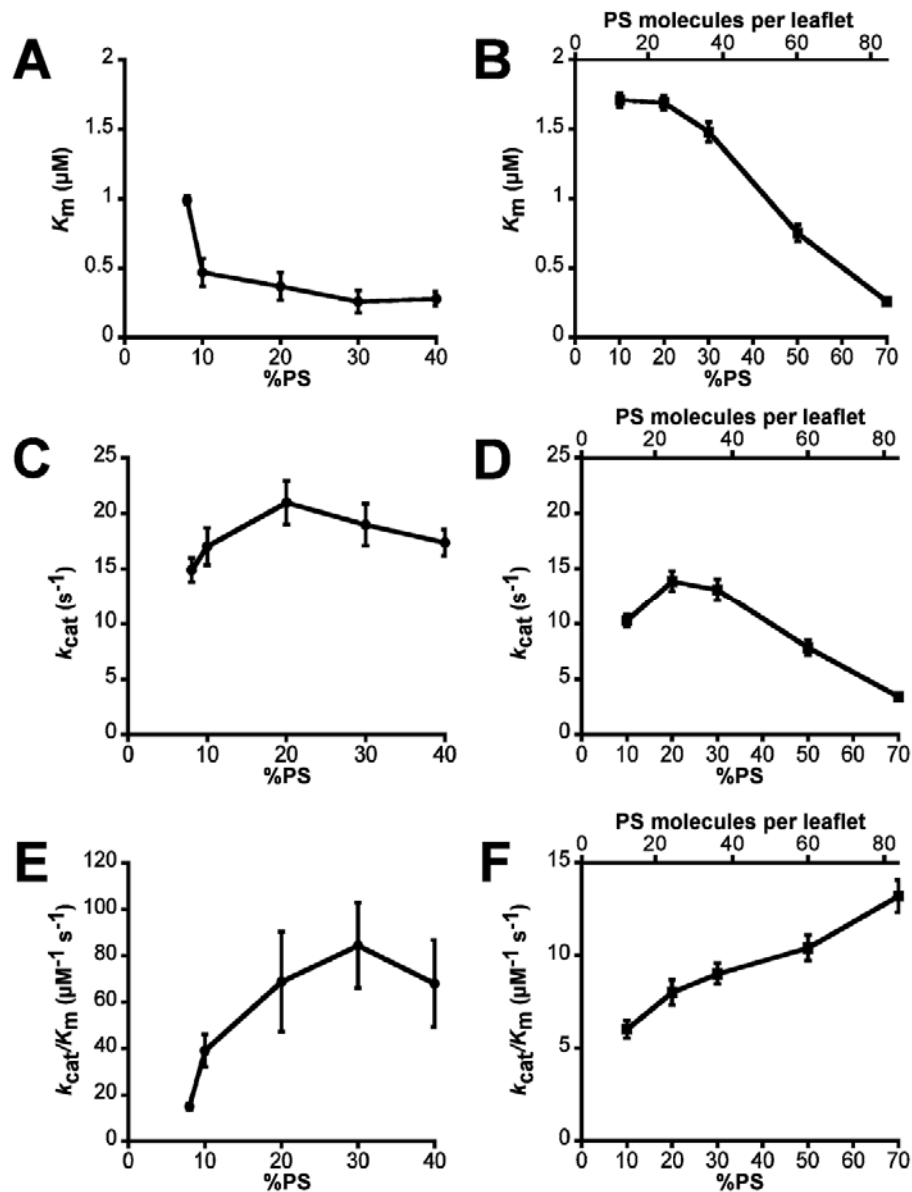
Figure 4.5   The local PS environment modulates prothrombin activation by prothrombinase. The following kinetic constants were measured for prothrombin activation by prothrombinase: K_m using liposomes *(A)* or 10.8 nm-diameter bilayer Nanodiscs *(B)*; k_{cat} using liposomes *(C)* or 10.8 nm-diameter bilayer Nanodiscs *(D)*; and k_{cat}/K_m using liposomes *(E)* or 10.8 nm-diameter bilayer Nanodiscs *(F)*. Data represent mean ± S.E. (*n* = 3). The *upper x axes* in *B*, *D*, and *F* represent the calculated number of PS molecules/leaflet, with mol % of PS indicated on the *lower x axes*. Under our experimental conditions rates of prothrombin activation were essentially undetectable in the absence of phospholipids or while using liposomes or Nanodiscs containing 100% PC, precluding their inclusion in this figure.

4.6   REFERENCES

1. Mann KG. The assembly of blood clotting complexes on membranes. *Trends in Biochemical Sciences* 1987; **12:** 229-233.

2. Mann KG. How much factor V is enough? *Thromb Haemost* 2000; **83:** 3-4.

3. Zwaal RF. Membrane and lipid involvement in blood coagulation. *Biochim Biophys Acta* 1978; **515:** 163-205.

4. Mann KG, Nesheim ME, Church WR, Haley P, Krishnaswamy S. Surface-dependent reactions of the vitamin K-dependent enzyme complexes. *Blood* 1990; **76:** 1-16.

5. Mann KG, Jenny RJ, Krishnaswamy S. Cofactor proteins in the assembly and expression of blood clotting enzyme complexes. *Annu Rev Biochem* 1988; **57:** 915-956.

6. Castellino FJ. Human Protein C and Activated Protein C - Components of the Human Anticoagulation System. *Trends in Cardiovascular Medicine* 1995; **5:** 55-62.

7. Haverstick DM, Glaser M. Visualization of Ca2+-induced phospholipid domains. *Proc Natl Acad Sci U S A* 1987; **84:** 4475-4479.

8. Yang L, Glaser M. Formation of membrane domains during the activation of protein kinase C. *Biochemistry* 1996; **35:** 13966-13974.

9. Shaw AW, McLean MA, Sligar SG. Phospholipid phase transitions in homogeneous nanometer scale bilayer discs. *FEBS Lett* 2004; **556:** 260-264.

10. Denisov IG, McLean MA, Shaw AW, Grinkova YV, Sligar SG. Thermotropic phase transition in soluble nanoscale lipid bilayers. *J Phys Chem B* 2005; **109:** 15580-15588.

11. Denisov IG, Grinkova YV, Lazarides AA, Sligar SG. Directed self-assembly of monodisperse phospholipid bilayer Nanodiscs with controlled size. *J Am Chem Soc* 2004; **126:** 3477-3487.

12. Bayburt TH, Sligar SG. Single-molecule height measurements on microsomal cytochrome P450 in nanometer-scale phospholipid bilayer disks. *Proc Natl Acad Sci U S A* 2002; **99:** 6725-6730.

13. Shaw AW, Pureza VS, Sligar SG, Morrissey JH. The local phospholipid environment modulates the activation of blood clotting. *J Biol Chem* 2007; **282:** 6556-6563.

14. Terrettaz S, Stora T, Duschl C, Vogel H. Protein binding to supported lipid membranes: investigation of the cholera toxin-ganglioside interaction by simultaneous impedance spectroscopy and surface plasmon resonance. *Langmuir* 1993; **14:** 2573-2576.

15. Heyse S, Vogel H, Sanger M, Sigrist H. Covalent attachment of functionalized lipid bilayers to planar waveguides for measuring protein binding to biomimetic membranes. *Protein Sci* 1995; **4:** 2532-2544.

16. Brufatto N, Nesheim ME. Analysis of the kinetics of prothrombin activation and evidence that two equilibrating forms of prothrombinase are involved in the process. *J Biol Chem* 2003; **278:** 6755-6764.

17. Krishnaswamy S, Mann KG, Nesheim ME. The prothrombinase-catalyzed activation of prothrombin proceeds through the intermediate meizothrombin in an ordered, sequential reaction. *J Biol Chem* 1986; **261:** 8977-8984.

18. Mizuno H, Fujimoto Z, Atoda H, Morita T. Crystal structure of an anticoagulant protein in complex with the Gla domain of factor X. *Proc Natl Acad Sci U S A* 2001; **98:** 7230-7234.

19. Adams TE, Hockin MF, Mann KG, Everse SJ. The crystal structure of activated protein C-inactivated bovine factor Va: Implications for cofactor function. *Proc Natl Acad Sci U S A* 2004; **101:** 8918-8923.

20. Hathcock JJ, Rusinova E, Gentry RD, Andree H, Nemerson Y. Phospholipid regulates the activation of factor X by tissue factor/factor VIIa (TF/VIIa) via substrate and product interactions. *Biochemistry* 2005; **44:** 8187-8197.

21. Majumder R, Wang J, Lentz BR. Effects of water soluble phosphotidylserine on bovine factor Xa: functional and structural changes plus dimerization. *Biophys J* 2003; **84:** 1238-1251.

22. Chattopadhyay R, Iacob R, Sen S, Majumder R, Tomer K, Lentz B. Functional and Structural Characterization of Factor Xa Dimer in Solution. *Biophysical Journal* 2009; **96:** 974-986.

23. Pusey ML, Mayer LD, Wei GJ, Bloomfield VA, Nelsestuen GL. Kinetic and hydrodynamic analysis of blood clotting factor V-membrane binding. *Biochemistry* 1982; **21:** 5262-5269.

24. Pusey ML, Nelsestuen GL. Membrane binding properties of blood coagulation Factor V and derived peptides. *Biochemistry* 1984; **23:** 6202-6210.

25. Tracy PB, Mann KG. Prothrombinase complex assembly on the platelet surface is mediated through the 74,000-dalton component of factor Va. *Proc Natl Acad Sci U S A* 1983; **80:** 2380-2384.

26. Koppaka V, Lentz BR. Binding of bovine factor Va to phosphatidylcholine membranes. *Biophys J* 1996; **70:** 2930-2937.

27. Tracy PB, Eide LL, Bowie EJ, Mann KG. Radioimmunoassay of factor V in human plasma and platelets. *Blood* 1982; **60:** 59-63.

28. Krishnaswamy S, Mann KG. The binding of factor Va to phospholipid vesicles. *J Biol Chem* 1988; **263:** 5714-5723.

29. Schroit AJ, Zwaal RF. Transbilayer movement of phospholipids in red cell and platelet membranes. *Biochim Biophys Acta* 1991; **1071:** 313-329.

30. Rosing J, Tans G, Govers-Riemslag JW, Zwaal RF, Hemker HC. The role of phospholipids and factor Va in the prothrombinase complex. *J Biol Chem* 1980; **255:** 274-283.

31. Nesheim ME, Eid S, Mann KG. Assembly of the prothrombinase complex in the absence of prothrombin. *J Biol Chem* 1981; **256:** 9874-9882.

32. Nesheim ME, Tracy RP, Mann KG. "Clotspeed," a mathematical simulation of the functional properties of prothrombinase. *J Biol Chem* 1984; **259:** 1447-1453.

33. Gerads I, Govers-Riemslag JW, Tans G, Zwaal RF, Rosing J. Prothrombin activation on membranes with anionic lipids containing phosphate, sulfate, and/or carboxyl groups. *Biochemistry* 1990; **29:** 7967-7974.

34. Govers-Riemslag JW, Janssen MP, Zwaal RF, Rosing J. Prothrombin activation on dioleoylphosphatidylcholine membranes. *Eur J Biochem* 1994; **220:** 131-138.

CHAPTER 5

CONCLUSIONS

5.1   SUMMARY

Blood coagulation requires the membrane assembly of protein complexes composed of catalytic and regulatory subunits. Damaged cells or platelets can dramatically influence the catalytic efficiencies of these membrane-bound proteases through increased exposure of anionic phospholipids such as PS on the outer leaflet of the plasma membrane. In the presence of Ca^{2+}, PS can spontaneously cluster into membrane microdomains upon which phospholipid-binding proteins may preferentially assemble. It therefore seems likely that blood clotting reactions occur on membrane surfaces containing very high amounts of PS in their immediate vicinities, which may result from both Ca^{2+} and the PS-binding properties of the proteins themselves. Thus, local variations in the nanoenvironment immediately surrounding these complexes may dramatically alter their activities. Unfortunately when using even simple model membranes, it is very difficult to define the phospholipid composition immediately surrounding these membrane-bound complexes and their substrates. In particular, when using liposomes or other model membranes, this parameter is typically not under experimental control.

For this reason, the membrane composition in the immediate vicinity of blood clotting reactions is largely unknown. I approached this problem by using a unique system of stable phospholipid bilayers of defined size as a platform for

studying membrane-protein interactions. These "Nanodiscs" are soluble, nanometer-scale bilayers that are encircled and stabilized by a protein called MSP. By assembling the constituent proteins of certain blood clotting complexes on these submicroscopic bilayers, the long-range recruitment of anionic phospholipids that occurs in larger phospholipid systems such as liposomes can be circumvented, and the identity and contribution of the membrane in the direct vicinity of these complexes can be more clearly defined.

Before conducting detailed studies with membrane-bound proteins of blood coagulation on Nanodiscs however, it was first necessary to assemble and characterize the Nanodisc system. Secondly, in order to study the initiation of blood coagulation by TF, it was also necessary to incorporate TF into the Nanodisc bilayer. Focusing my experiments on Nanodiscs with bilayers having diameters of 7.7 and 10.8 nm, my results showed that Nanodiscs with 8 nm-diameter bilayers contained a mean of 67 ± 1 phospholipid molecules per bilayer leaflet and had final proportions of PC and PS that were faithfully preserved throughout the assembly process. Likewise, Nanodiscs with 10.8 nm-diameter bilayers were found to contain a mean of 120 ± 4 phospholipid molecules per leaflet. Except for extreme circumstances, Nanodisc species containing PCPS bilayers are stable in physiological amounts of Ca^{2+}. Moreover, active membrane-bound TF has been successfully reconstituted into 8 nm-diameter Nanodiscs. These TF-Nanodiscs have a stoichiometry of 1.02 TF molecules per Nanodisc and exhibit considerable procoagulant activity. Overall, these results

validate the use of these bilayers as tightly-controlled membrane surfaces upon which to control, assemble and study the components of the blood coagulation cascade at the nanoscale.

Using Nanodiscs, I investigated how altering the PS content in the immediate environment surrounding the TF·VIIa complex controls the catalytic efficiency toward its membrane-binding substrate, fX. I found that as the PS content of the nanobilayers increased, fX bound these membranes in a saturable and concentration-dependent manner. Furthermore, as PS increased, both the affinity and the amount of fX bound to these membranes increased concordantly. Through the same system, I also showed that full proteolytic activity of the TF·VIIa complex requires extremely high local concentrations of anionic phospholipids, and furthermore that a large membrane-bound pool of its substrate, fX, is not required to support sustained catalysis. These findings provided new insights into the initiation of thrombosis; the event that triggers the death of most people.

Next, I investigated how altering the PS content of the membrane surface surrounding Va·Xa complex controls its catalytic efficiency toward its membrane-binding substrate, prothrombin. I found that the number of binding sites for factors Va, Xa and prothrombin increased almost linearly with the number of PS molecules per nanobilayer. Effects on binding affinity were more complex: K_d values for binding of factor Xa or prothrombin to nanobilayers decreased monotonically with increasing PS content, while the K_d for factor Va-nanobilayer

97

binding showed a biphasic dependence on PS content. K_m for prothrombin

activation decreased correspondingly as the PS content of nanobilayers

increased, while k_{cat} exhibited a biphasic dependence on PS content. The k_{cat}/K_m

for prothrombin activation by prothrombinase assembled on nanobilayers

increased almost linearly with PS content. These results reveal how anionic

phospholipids in the direct vicinity (*i.e.,* within a few nanometers) of the final

membrane-bound complex of blood coagulation regulates its assembly and

function.

Many blood coagulation serine proteases and their subsequent

protease:cofactor complexes have evolved binding sites to regulate their

functions. At the fundamental level, these "exosites" may be anywhere in the

vicinity of the complex, yet by definition lie outside the active site. In fact,

exosites may be located on the protease, the protein cofactor, or both. In this

project, I have described how the TF·VIIa and Va·Xa complexes use anionic

phospholipids within their immediate vicinity to mediate the binding affinity of their

constituent proteins and substrates. In light of these findings, I propose that the

PS molecules located within nanometers of these complexes serve as critical

exosites to regulate their assemblies and function.

5.2   FUTURE DIRECTIONS

5.2.1 Lipid-Mediated Regulation of Blood Coagulation Complexes

I have demonstrated that the TF·VIIa enzyme complex can efficiently

activate its natural protein substrate, fX, even when this membrane-bound

enzyme complex is confined to a nanoscale lipid bilayer consisting of only ~67

phospholipid molecules per leaflet (Fig. 3.4). My results with TF-liposomes have

showed that k_{cat} values increased as the percentage of PS was elevated,

paralleling the PS dependence of fX binding to Nanodiscs (Fig. 3.2B). At very

high concentrations of PS, however, TF-Nanodiscs did not exhibit this behavior.

Instead, when the PS composition in Nanodiscs was raised to an extremely high

amount, product turnover slowed. Notably, this phenomenon also occurs with

the Va·Xa complex (see Fig 4.5).

Hathcock *et al.*, [1,2], have proposed that removal of product (fXa) from

the vicinity of the TF:VIIa complex by lateral diffusion on the membrane surface is

likely the rate-limiting process controlling the apparent k_{cat} of this reaction. It can

be further speculated that this same mechanism may be occurring with the Va·Xa

complex as well. It is possible that product removal from these membrane-bound

blood coagulation complexes may be less effective when they are constrained

within nanoscale bilayers, and especially when the PS composition of the bilayer

is very high.

This unusual phenomenon may be because the tiny membrane surface

within the Nanodisc must rely on continuous binding of membrane-bound

substrate to, and dissociation of membrane-bound product from the nanobilayer

to allow sustained rates of substrate activation. Turnover of substrate is

therefore dependent upon dissociation of product from the membrane in order to

provide room for new substrate molecules to bind within a few nm of the blood

coagulation protein complex. As the PS composition of the nanobilayer

increases, however, so do the binding affinities of substrates and products for the

membrane surface. Moreover, if the product has a higher affinity for PS

membranes compared to the substrate, the product may effectively inhibit this

reaction.

Investigating if the nascent product of these complexes competitively

inhibits the catalysis of their respective substrates may yield additional insight as

to how the blood coagulation cascade is regulated. Through the Nanodisc

system, TF·VIIa or Va·Xa-catalyzed reactions can be finely examined as a

function of bilayer size and PS content at a level never before seen. Using, for

example, a product of the respective reactions as a competitor to inhibit or rescue

the turnover rate of the enzyme-cofactor complex. The use of stopped-flow may

also be valuable to further investigate rate of substrate association and product

dissociation to and from these membrane complexes.

5.2.2 Phosphatidylethanolamine-Mediated Enhancement of Clotting Factor Activity

To great effect, many *in vitro* studies involving blood coagulation

complexes have used mixtures of net neutral and anionic phospholipids in

liposome-based systems that recapitulate the stimulatory effects of their natural

counterparts (*e.g.,* activated platelets and damaged endothelial cells). Notably,

PS is accepted as the most effective surface in supporting catalysis [3]. Studies

by the Morrissey group have subsequently demonstrated that

phosphatidylethnolamine (PE) can synergize with low levels of PS to promote fX activation by the TF·VIIa complex comparable to liposomal preparations that have much higher PS content [4]. The mechanism for this synergy is not incompletely understood and notably applies not only to TF·VIIa, but to other membrane-bound complexes of blood coagulation.

One hypothesis for this phenomenon is that due to its tendency to produce hexagonal-shaped bilayers, PE may induce the clustering of PS microdomains on liposomal surfaces. As such, this phenomenon promotes more efficient substrate utilization from membrane-bound blood coagulation complexes. Since Nanodiscs are such small bilayers, they may essentially represent membrane microdomains themselves, rendering PE-induced clustering of PS unlikely. When comparing the PSPE-dependence of fX activation by TF·VIIa on Nanodiscs and liposomes, absence of PSPE synergy in Nanodiscs may support to this idea. An alternate hypothesis is that PE, along with PS, represents yet another binding site for membrane-binding procoagulant proteins. As such, if synergy is indeed present in PEPS-containing Nanodiscs, the effect of PE on the binding affinity of the component clotting factors to Nanodiscs may be measured via SPR and other binding experiments. These experiments can be further expanded to other natural phospholipids, such as phosphatidylinositol and phosphatidylglycerol, which have been found to affect the function of blood clotting proteins.

5.2.3 Assembly and Function of Other Membrane-Bound Hemostatic Complexes on Nanodiscs

Through this project, I have shown that Nanodiscs provide a bilayer of defined size and phospholipid composition that may be effectively used as an experimental membrane surface upon which to assemble and study the components of both the TF·VIIa and Va·Xa complexes. A logical expansion of this work is to investigate other membrane-bound protease complexes involved in hemostasis. Two notable candidates are the intrinsic tenase and the thrombin·thrombomodulin complexes. The intrinsic tenase complex is another physiological activator of fX. It is composed of the serine protease factor IXa (fIXa), and its protein cofactor factor VIIIa (fVIIIa). fIXa is yet another vitamin K dependent serine protease (much like fVIIa and fXa), and fVIIIa greatly resembles fVa in structure and function. The thrombin-thrombomodulin complex, on the other hand, activates a serine protease zymogen called protein C, ultimately leading to clot dissolution. Notably, thrombomodulin is an integral membrane protein like TF and must be incorporated into a suitable membrane for optimal activity. Experiments concerning these complexes may be conducted in a manner very similar to the present work, but should take account the different properties of the constituent proteins involved in each complex.

5.2.4 TF-Nanodiscs as Therapeutic Hemostatic Agents.

TF embedded within Nanodiscs (TF-Nanodiscs) demonstrated appreciable procoagulant activity. Moreover, it was found that the composition of the phospholipid membrane in the immediate vicinity of TF (and other procoagulant

proteins) can dramatically influence its function. In many ways, these results provide greater insight into how the initiation of blood coagulation may be induced and controlled both *in vitro* and *in vivo*. A natural extension of this project may therefore be the development and application of TF-Nanodiscs of superior solubility and stability for the delivery of TF. Clinically, TF-Nanodiscs could function as novel, highly potent hemostatic agents and tumor-targeting agents.

The physical properties of the Nanodisc itself make it an excellent candidate for *in vivo* protein delivery. For instance, because they were originally derived from and resemble natural lipoproteins in the body, Nanodiscs may demonstrate reduced toxicity and immunoreactivity. Their readily modifiable structural properties could enable the attachment of targeting molecules or of solid supports to the MSP, the phospholipid bilayer, or directly on TF itself. Moreover, their small size may enable diffusion through small capillaries that larger particles cannot otherwise traverse, and their homogeneity may aid in ensuring controlled dosages. Nanodiscs can furthermore be inexpensively produced in large quantities and in a relatively short amount of time.

Existing hemostatic agents for the cessation of excessive bleeding are generally composed of formulations that are weak activators of blood coagulation. Presently, collagen and oxidized cellulose are commonly used in surgery to prevent bleeding [5,6]. These formulations work as hemostatic agents by promoting the activation of platelets, and are often supplemented with

thrombin. However, as one of the last enzymes in the blood clotting cascade,

thrombin must be used in very high concentrations. Fibrin sealants composed of

fibrinogen and thrombin are also commonly used [7]. These processes invariably

take advantage of the latter part of the procoagulant pathway, and are inefficient

initiators of blood coagulation. On the other hand, membrane-bound TF is the

strongest activator of the blood coagulation cascade, and TF-Nanodiscs exhibit

considerable procoagulant activity. As such, for treatment of excessive bleeding

due to surgery, trauma, or deficiencies in the clotting system, TF-Nanodiscs may

represent superior formulations for inducing the cessation of blood loss.

Additionally, the scaffold protein of TF-Nanodiscs may be crosslinked and

immobilized onto a solid support such as collagen or Dacron. This will prevent

TF from migrating freely or being washed away by hemorrhaging blood, thereby

increasing the local concentration of TF at the desired site.

Solid tumors induce angiogenesis in order to sustain their rapid growth.

The infarction of tumor vasculature can effectively destroy many critical, blood-

dependent layers of a tumor. Therefore, antivascular therapy for the targeting

and infarction of tumors has been a very promising research topic for many

years. The delivery of non-membrane bound, soluble TF (sTF) to the vascular

bed of tumors, for example, has been tested in a variety of model studies [8-11].

Since it is missing a suitable membrane surface, however, sTF contains activity

that is orders of magnitude less than membrane-bound TF. TF-Nanodiscs may

potentially have superior efficacy for the infarction of tumors. For future work on

vascular tumor delivery of TF-Nanodiscs, an improved formulation of TF-

Nanodiscs with optimized enzymatic activity may be made. For vascular

targeting, a fusion protein containing, for example, the ED-B domain of

fibronectin may be attached to TF and inserted into Nanodiscs. The ED-B

domain is a marker for tumoral vasculature expressed in the majority of

aggressive solid tumors but is undetectable in normal tissues. TF-Nanodiscs

containing the ED-B domain may therefore be used to target tumor vasculature in

experimental mice. As the amino acid sequence of ED-B is identical in mice,

rats, dogs, and humans [11], it is an excellent initial candidate for interspecies

experiments that may eventually culminate in studies in humans.

5.3   REFERENCES

1. Hathcock JJ, Rusinova E, Gentry RD, Andree H, Nemerson Y. Phospholipid regulates the activation of factor X by tissue factor/factor VIIa (TF/VIIa) via substrate and product interactions. *Biochemistry* 2005; **44:** 8187-8197.

2. Hathcock JJ, Rusinova E, Andree H, Nemerson Y. Phospholipid surfaces regulate the delivery of substrate to tissue factor:VIIa and the removal of product. *Blood Cells Mol Dis* 2006; **36:** 194-198.

3. Mann KG, Jenny RJ, Krishnaswamy S. Cofactor proteins in the assembly and expression of blood clotting enzyme complexes. *Annu Rev Biochem* 1988; **57:** 915-956.

4. Neuenschwander PF, Bianco-Fisher E, Rezaie AR, Morrissey JH. Phosphatidylethanolamine augments factor VIIa-tissue factor activity: enhancement of sensitivity to phosphatidylserine. *Biochemistry* 1995; **34:** 13988-13993.

5. Sirlak M, Eryilmaz S, Yazicioglu L, Kiziltepe U, Eyileten Z, Durdu MS, Tasoz R, Eren NT, Aral A, Kaya B, Akalin H. Comparative study of microfibrillar collagen hemostat (Colgel) and oxidized cellulose (Surgicel)

in high transfusion-risk cardiac surgery. *J Thorac Cardiovasc Surg* 2003; **126:** 666-670.

6. Schonauer C, Tessitore E, Barbagallo G, Albanese V, Moraci A. The use of local agents: bone wax, gelatin, collagen, oxidized cellulose. *Eur Spine J* 2004; **13 Suppl 1:** S89-S96.

7. Schexneider KI. Fibrin sealants in surgical or traumatic hemorrhage. *Curr Opin Hematol* 2004; **11:** 323-326.

8. Huang X, Molema G, King S, Watkins L, Edgington TS, Thorpe PE. Tumor infarction in mice by antibody-directed targeting of tissue factor to tumor vasculature. *Science* 1997; **275:** 547-550.

9. Ran S, Gao B, Duffy S, Watkins L, Rote N, Thorpe PE. Infarction of solid Hodgkin's tumors in mice by antibody-directed targeting of tissue factor to tumor vasculature. *Cancer Res* 1998; **58:** 4646-4653.

10. Rippmann JF, Pfizenmaier K, Mattes R, Rettig WJ, Moosmayer D. Fusion of the tissue factor extracellular domain to a tumour stroma specific single-chain fragment variable antibody results in an antigen-specific coagulation-promoting molecule. *Biochem J* 2000; **349 Pt 3:** 805-812.

11. Nilsson F, Kosmehl H, Zardi L, Neri D. Targeted delivery of tissue factor to the ED-B domain of fibronectin, a marker of angiogenesis, mediates the infarction of solid tumors in mice. *Cancer Res* 2001; **61:** 711-716.

VINCENT S. PUREZA

1901 SOUTHWOOD DRIVE • CHAMPAIGN, IL 61820
PHONE: (209) 878–7392 • E-MAIL: VPUREZA@ILLINOIS.EDU

EDUCATION

2002 – 2009	University of Illinois at Urbana-Champaign *PhD in Biochemistry, 2009* *MD, 2012 (anticipated graduation)*	Urbana, IL
1996 – 2001	California State University at Northridge *BA in Honors Biology, 2001*	Northridge, CA

SELECTED HONORS

2009	Baxter Innovation Award
2006 – 2008	AHA Predoctoral Research Fellowship
1999 – 2001	NIH MARC Research Fellowship
2001	Donald E Bianchi Award for Best Undergraduate Research
2001	CSUN Honors in Biology
2001	CSUN Honors in General Education
2001	Endocrine Society's Outstanding Project Award

RESEARCH EXPERIENCE

2003 – 2009	University of Illinois at Urbana-Champaign	Urbana, IL

James Morrissey, PhD
    Blood coagulation reactions on nanoscale membrane surfaces

1999 – 2001	California State University at Northridge	Northridge, CA

Aïda Metzenberg, CGC, PhD
    Mutation analysis of Happle Syndrome
    Subcellular localization of the Barth protein

Summer 2000	University of California at San Francisco	San Francisco, CA

Joanne Engel, MD, PhD
    Growth phase-dependent apoptosis of Pseudomonas *in HeLa cells*

PUBLICATIONS

Pureza VS, Sligar SG, and Morrissey JH. Influence of the local phospholipid nanoenvironment on prothrombinase function. *In preparation*.

Morrissey JH, Pureza V, Davis-Harrison RL, Sligar SG, Rienstra CM, Kijac AZ, Ohkubo YZ and Tajkhorshid E. Protein-membrane interactions: blood clotting on nanoscale bilayers. *Journal of Thrombosis and Haemostasis*, 7 (Suppl. 1):169-172, 2009.

Morrissey JH, Pureza V, Davis-Harrison RL, Sligar SG, Ohkubo YZ and Tajkhorshid E. Blood clotting reactions on nanoscale phospholipid bilayers. *Thrombosis Research*, 122 (Suppl. 1): S26-26, 2008.

Shaw AW*, Pureza VS*, Sligar SG, and Morrissey JH. The local phospholipid environment modulates the activation of blood clotting. *Journal of Biological Chemistry*, 282(9): 6556-6563, 2007. *Both authors contributed equally to the manuscript.

Morrissey JH, Sligar SG, and Pureza VS. Tissue factor compositions and methods. *US patent application*, Serial Number 11/259,950, October 2005.

Morrissey JH, Sligar SG, and Pureza VS. Tissue factor compositions and methods. *PCT patent application*, Serial Number PCT/US2005/38781, October 2005.

Aughton DJ, Kelley RI, Metzenberg A, Pureza V, and Pauli RM. X-linked dominant chondrodysplasia punctata (CDPX2) caused by single-gene mosaicism in a male. *American Journal of Medical Genetics*, 116A: 255–260, 2003.

Herman G, Kelley RI, Pureza V, Smith D, Kopacz K, Pitt J, Sutphen R, Sheffield LJ, and Metzenberg A. Characterization of mutations in 22 females with X-linked dominant chondrodysplasia punctata (Happle syndrome). *Genetics in Medicine,* 4(6): 434–438, 2002.

Pureza V. Gene mapping by biochemistry: Mutation analysis of chondrodysplasia punctata in patients with elevated sterol levels. *Undergraduate honors thesis, California State University at Northridge*, 2001.